NUSC Technical Memorandum 841208
31 December 1984

Under-Ice Roughness: Shot Noise Model

Albert H. Nuttall
Surface Ship Sonar Department

Naval Underwater Systems Center
Newport, Rhode Island/New London, Connecticut

Report Documentation Page

Form Approved
OMB No. 0704-0188

1. REPORT DATE	2. REPORT TYPE	3. DATES COVERED
31 DEC 1984	**Technical Memo**	**31-12-1984 to 31-12-1984**

4. TITLE AND SUBTITLE
Under-Ice Roughness: Shot Noise Model

5a. CONTRACT NUMBER

5b. GRANT NUMBER

5c. PROGRAM ELEMENT NUMBER

6. AUTHOR(S)
Albert Nuttall

5d. PROJECT NUMBER
A65090 and A74205

5e. TASK NUMBER

5f. WORK UNIT NUMBER

7. PERFORMING ORGANIZATION NAME(S) AND ADDRESS(ES)
Naval Underwater Systems Center,New London,CT,06320

8. PERFORMING ORGANIZATION REPORT NUMBER
TM No. 841208

9. SPONSORING/MONITORING AGENCY NAME(S) AND ADDRESS(ES)

10. SPONSOR/MONITOR’S ACRONYM(S)

11. SPONSOR/MONITOR’S REPORT NUMBER(S)

12. DISTRIBUTION/AVAILABILITY STATEMENT
Approved for public release; distribution unlimited

13. SUPPLEMENTARY NOTES
NUWC2015

14. ABSTRACT
The one-dimensional roughness of an under-ice profile of elliptical bosses is modeled in the time domain by a shot noise process of elliptical pulses of random amplitude, duration, and time of occurrence. A sample realization of 8000 data points is generated and plotted for visual comparison with experimental under-ice data. Also, theoretical and simulation results for the power density spectrum, the autocorrelation function, the characteristic function, the cumulative distribution function, and the probability density function of the shot noise process are plotted and compared.

15. SUBJECT TERMS
ZR000-01; Evaluation of Incoherent Field in the Arctic Environment; ZR0000101; Applications of Statistical Communication Theory to Acoustic Signal Processing; under-ice; elliptical bosses

16. SECURITY CLASSIFICATION OF:			17. LIMITATION OF ABSTRACT	18. NUMBER OF PAGES	19a. NAME OF RESPONSIBLE PERSON
a. REPORT	b. ABSTRACT	c. THIS PAGE			
unclassified	**unclassified**	**unclassified**	**Same as Report (SAR)**	**58**	

TM No. 841208

cy 001

NAVAL UNDERWATER SYSTEMS CENTER

New London Laboratory

New London, Connecticut

UNDER-ICE ROUGHNESS: SHOT NOISE MODEL

Date: 31 December 1984

Prepared by: Albert H Nuttall

Albert H. Nuttall

Surface Ship Sonar

Department

Approved for public release; distribution unlimited

ABSTRACT

The one-dimensional roughness of an under-ice profile of elliptical bosses is modeled in the time domain by a shot noise process of elliptical pulses of random amplitude, duration, and time of occurrence. A sample realization of 8000 data points is generated and plotted for visual comparison with experimental under-ice data. Also, theoretical and simulation results for the power density spectrum, the autocorrelation function, the characteristic function, the cumulative distribution function, and the probability density function of the shot noise process are plotted and compared.

ADMINISTRATIVE INFORMATION

This memorandum was prepared under NUSC Project No. A65090, Subproject No. ZR000-01, "Evaluation of Incoherent Field in the Arctic Environment," Principal Investigator R.L. Deavenport, Code 3332, and under NUSC Project No. A75205, Subproject No. ZR0000101, "Applications of Statistical Communication Theory to Acoustic Signal Processing," Principal Investigator Dr. A.H. Nuttall, Code 33, Program Manager Gary Morton, Naval Material Command, MAT 05.

The author of this technical memorandum is located at the Naval Underwater Systems Center, New London, CT 06320.

INTRODUCTION

The under-ice profile has been observed to appear like a random collection of superposed elliptical bosses, each of random amplitude, length, and location. An analogous model in the time domain is shot noise composed of overlapping pulses of random amplitude, duration, and time of occurrence. Accordingly, we have generated a sample realization of a shot noise process for visual comparison with experimental under-ice data, and for possible corroboration of this model. The particular realization generated has 8000 data points, although the number of effectively-independent samples is far fewer, as will be demonstrated.

A number of analytical results for shot noise have been derived in the past [1]; however, they did not cover the case of random duration modulation. We have extended the analyses to include random durations (as well as random amplitudes and random time occurrences) and evaluated the spectrum of the shot noise process, as well as the autocorrelation function and the first-order characteristic function of the instantaneous amplitude. From the latter, the first-order probability density function and cumulative distribution function of shot noise have been evaluated via a generalized Laguerre expansion employing 32 cumulants or moments. Comparisons of all these theoretical results with the corresponding sample quantities, obtained from the 8000 data point realization above, reveal excellent agreement.

A REALIZATION OF A SHOT-NOISE PROCESS

Shot noise is characterized by a superposition of pulses, each located independently and uniformly on the time scale. A sample pulse is illustrated in figure 1. The time of occurrence t_k (center of symmetrical pulse, for

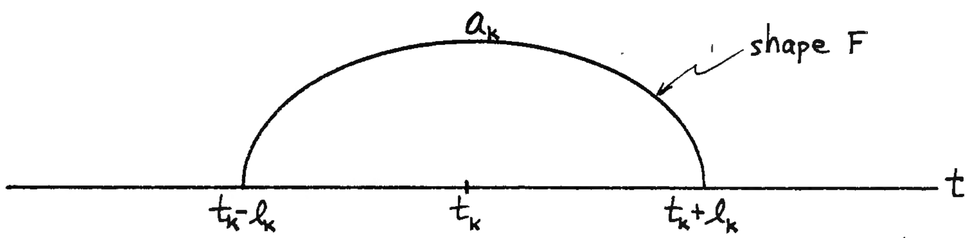

Figure 1. Sample Pulse of Shot Noise

example) is uniformly distributed in time t, with an average number of pulses per second, ν. The amplitude a_k and half-duration ℓ_k of an individual pulse are also all independent and are each identically randomly-distributed with arbitrary probability density functions. Finally the fundamental pulse shape F in figure 1 is arbitrary.

A realization of shot noise is given by

$$I(t) = \sum_k a_k \, F\left(\frac{t-t_k}{\ell_k}\right) , \tag{1}$$

where the summation extends over all k. The particular data we generate here employs the following example; unscaled pulse shape F is circular:

$$F(x) = \left\{ \begin{matrix} \left(1-x^2\right)^{1/2} \text{ for } & |x| < 1 \\ 0 \quad \text{ for } & |x| > 1 \end{matrix} \right\} . \tag{2}$$

This pulse is continuous; however, it has cusps (infinite slope) at $x = \pm 1$. The reason for this selection will become apparent when we discuss the spectrum of shot noise process (1).

The amplitude probability density function for random variable a_k is Rayleigh,

$$p(a) = \frac{a}{\sigma_a^2} \exp\left(\frac{-a^2}{2\sigma_a^2}\right) U(a) , \tag{3}$$

and the duration probability density function for random variable ℓ_k is also Rayleigh,

$$p(\ell) = \frac{\ell}{\sigma_\ell^2} \exp\left(\frac{-\ell^2}{2\sigma_\ell^2}\right) U(\ell) . \tag{4}$$

Here, step function

$$U(x) = \left\{\begin{array}{l} 1 \text{ for } x > 0 \\ 0 \text{ for } x < 0 \end{array}\right\}. \tag{5}$$

The mean values of random variables a_k and ℓ_k are given respectively by

$$\overline{a} = \overline{a_k} = \left(\frac{\pi}{2}\right)^{1/2} \sigma_a , \quad \overline{\ell} = \overline{\ell_k} = \left(\frac{\pi}{2}\right)^{1/2} \sigma_\ell , \tag{6}$$

in terms of the parameters σ_a and σ_ℓ of probability density functions (3) and (4). Alternatively, the mean square values are given by

$$\overline{a^2} = \overline{a_k^2} = 2\sigma_a^2 , \quad \overline{\ell^2} = \overline{\ell_k^2} = 2\sigma_\ell^2 . \tag{7}$$

Three typical component pulses are depicted in figure 2, and can range from circular through various elongated elliptical shapes. The total length of an individual pulse is $L_k = 2\ell_k$. An important parameter of this time-

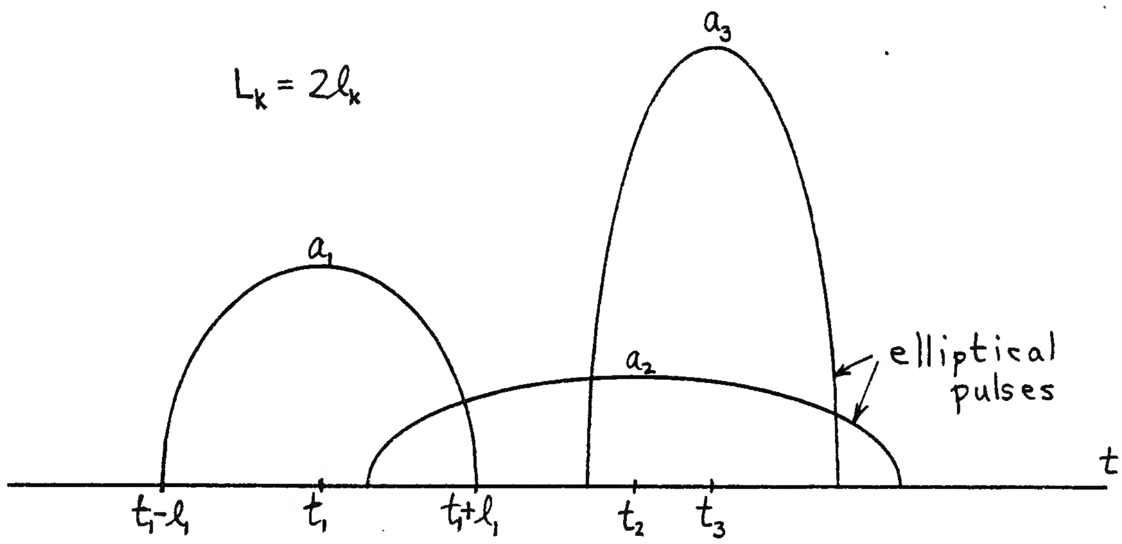

Figure 2. Three Component Pulses

limited pulse shape in figures 1 and 2 is the (dimensionless) overlap factor

$$\bar{L}_k \nu = 2\bar{\ell}_k \nu = 2\left(\frac{\pi}{2}\right)^{1/2} \sigma_\ell \nu \ . \tag{8}$$

This is the average number of pulses that are overlapping at any one instant of time, and is a partial measure of the applicability of the central limit theorem. A more meaningful measure are the cumulants; for probability density function (3) and pulse shape (2), the normalized third and fourth cumulants are

$$\frac{1.017}{(\bar{L}_k \nu)^{1/2}} \quad \text{and} \quad \frac{1.2}{\bar{\ell}_k \nu} \ , \tag{9}$$

respectively. In the sample realization generated here, the overlap factor in (8) was 6.2, leading to normalized cumulant values in (9) of .58 and .39, respectively. Since a Gaussian probability density function would lead to zero cumulants above second-order, the shot noise realization dealt with here is distinctly non-Gaussian.

In the three parts of figure 3, a realization of shot noise model (1) is given for parameter values

$$\sigma_a = 1 \text{ sec}, \quad \sigma_\ell = 20 \text{ sec}, \quad \nu = .124 \text{ pulses/sec}. \qquad (10)$$

The waveform (1) is sampled at unit time increments and connected by straight lines; thus the initial 100 data points illustrated in figure 3A have a jagged appearance for those component pulses with small ℓ_k, as for example at time instants 67-68. The larger duration pulses, like the one centered at t = 29, have a smoother appearance.

In figure 3B, the initial 1000 data points illustrate the very erratic character of shot noise; the waveform consists of some very sharp spiky pulses and other broader smooth components. The appearance of a downward trend in these 1000 data points is erased when the entire 8000 data point sequence is viewed in figure 3C. The possibility of shot noise process (1) reaching a zero value (when no pulses overlap) is confirmed by the waveform values near t = 6400.

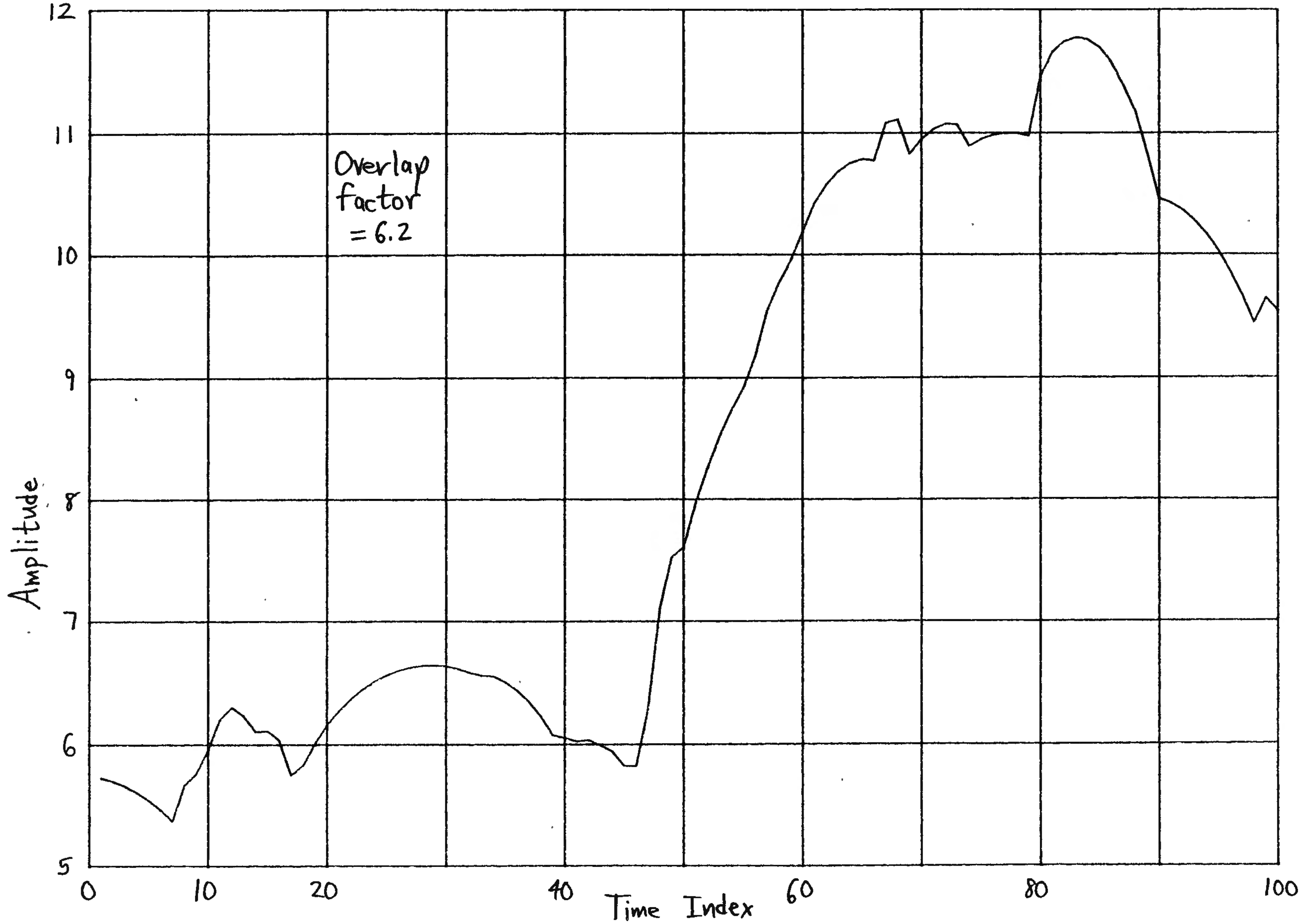

Figure 3A. Initial 100 Data Points

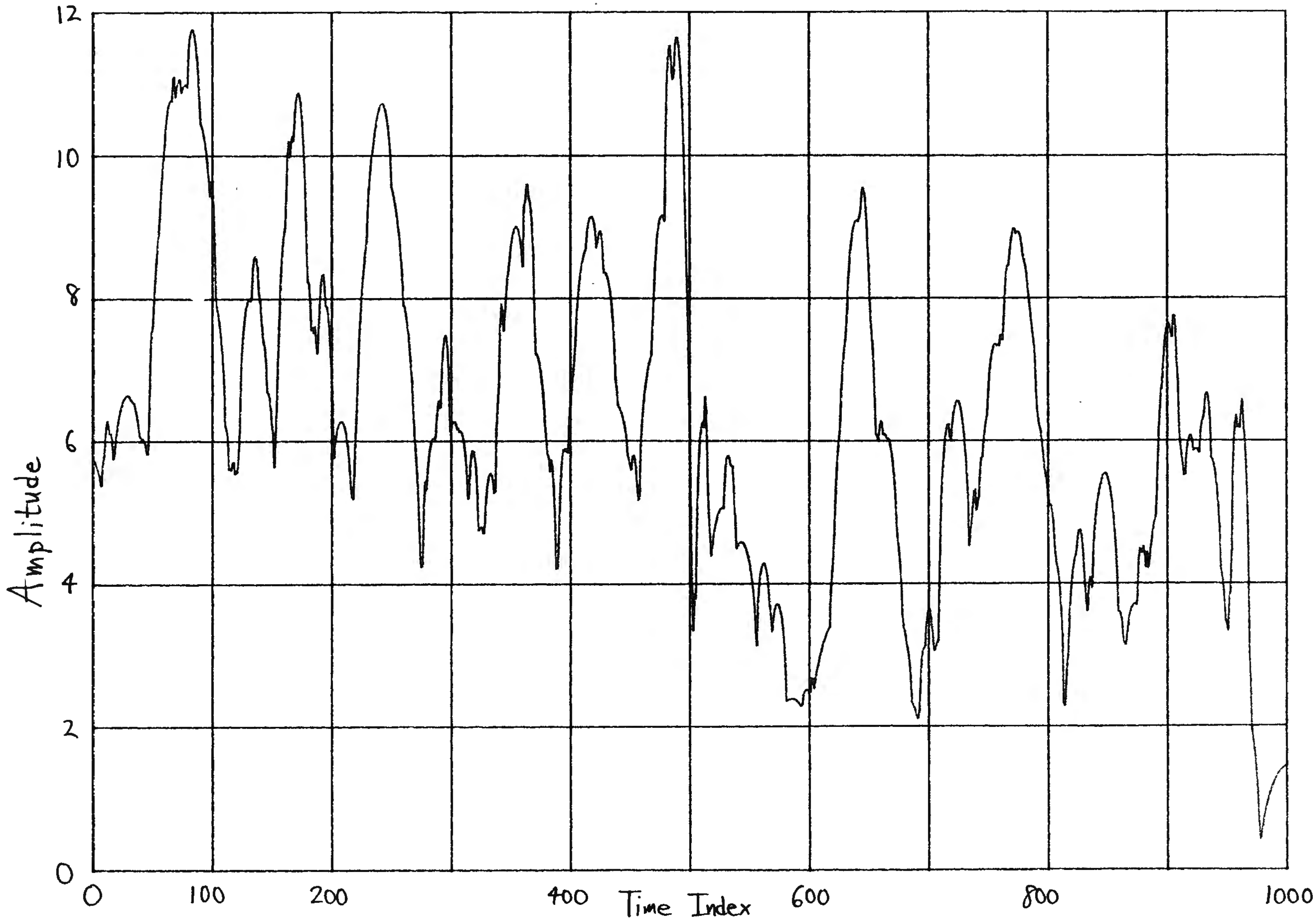

Figure 3B. Initial 1000 Data Points

TM No. 841208

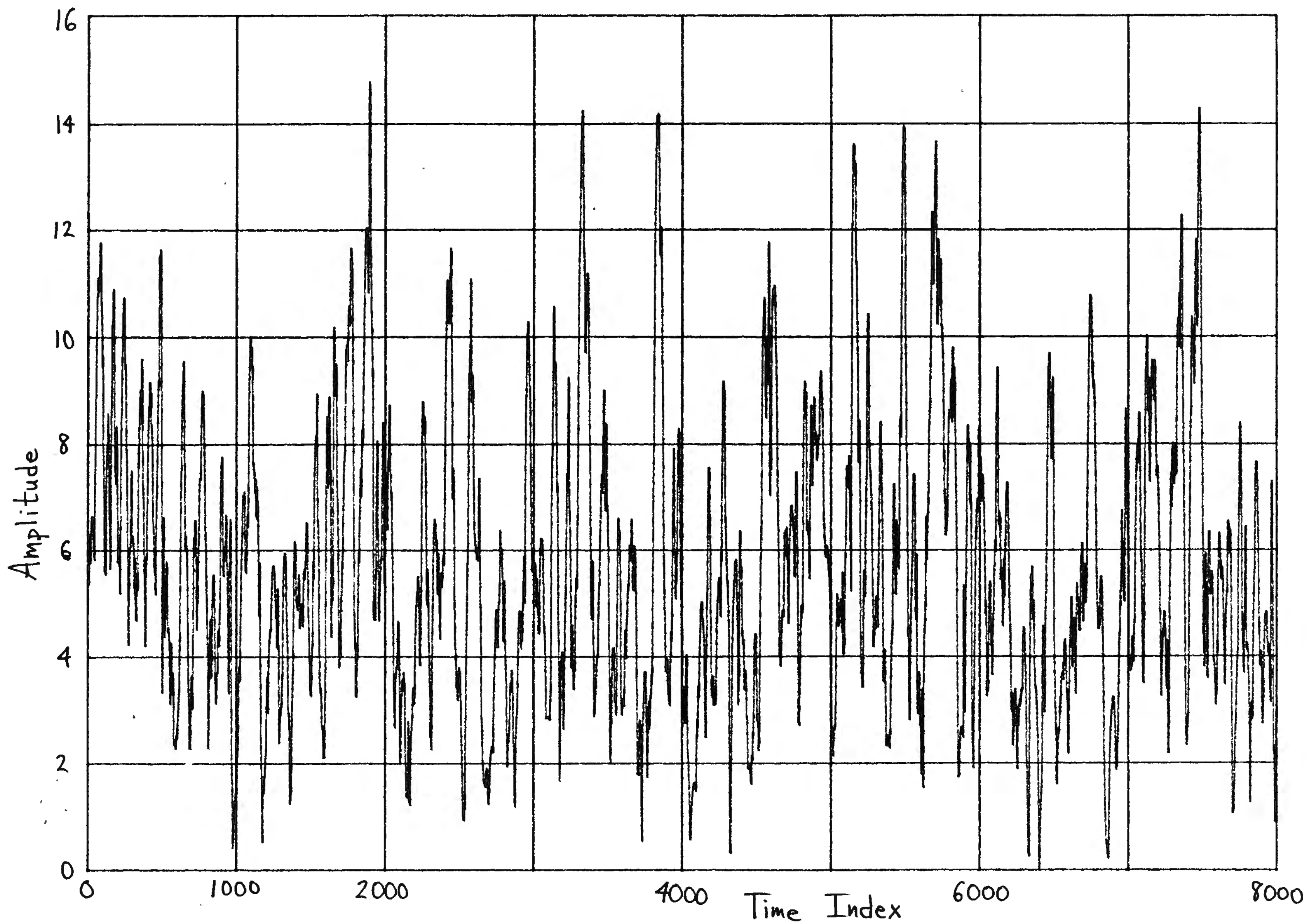

Figure 3C. Total Data Segment

CORRELATION AND SPECTRUM OF SHOT NOISE PROCESS

The derivations of the correlation and spectrum of the shot noise process (1) are given in appendix A; from (A-12), we have, in general, the correlation function at delay τ,

$$R_I(\tau) = \nu \, \overline{a^2} \int d\ell \; p(\ell)\ell \; \phi(\tau/\ell) + I_{dc}^2 \, , \tag{11}$$

where the dc component of I(t) is, from (A-13),

$$I_{dc} = \nu \, \overline{a} \, \overline{\ell} \int dx \; F(x) \, , \tag{12}$$

and

$$\phi(y) = \int dx \; F(x) \; F(x-y) \tag{13}$$

is the (aperiodic) correlation of an individual pulse F. (All integrals are over the range of non-zero integrand.)

Also, from (A-16), the general spectrum of process I(t) is, at frequency f,

$$G_I(f) = \nu \, \overline{a^2} \int d\ell \; p(\ell) \; \ell^2 \; \left|S(\ell f)\right|^2 + I_{dc}^2 \, \delta(f) \, , \tag{14}$$

where

$$S(f) = \int dx \; \exp(-i2\pi fx) \; F(x) \tag{15}$$

is the voltage density spectrum (Fourier transform) of pulse F. Thus $\left|S(f)\right|^2$ is the energy density spectrum corresponding to pulse F.

It should be observed that the entire probability density function $p(\ell)$ of half-duration random variable ℓ_k is required in order to evaluate the correlation or spectrum of shot noise. However, only the first two moments, $\overline{a}$ and $\overline{a^2}$, are required known about probability density function $p(a)$ of amplitude random variable a_k. The only way that the dc term I_{dc} can be zero is if random variable a_k has zero mean ($\overline{a} = 0$), or if pulse F has zero area ($S(0) = 0$).

Example

The example of interest here was given earlier in (2) and (4), namely a circular pulse F and a Rayleigh probability density function for random variable ℓ_k. The spectrum $G_I(f)$ in (14) is evaluated in (A-17) through (A-22), with the results

$$S(f) = \frac{J_1(2\pi f)}{2f}, \quad S(0) = \frac{\pi}{2},$$

$$I_{dc} = \left(\frac{\pi}{2}\right)^{3/2} \nu \, \overline{a} \, \sigma_\ell ,$$

$$G_I(f) = 2\pi^2 \, \nu \, \overline{a^2} \, \sigma_\ell^2 \, \frac{2 \exp(-z) \, I_1(z)}{z} + \left(\frac{\pi}{2}\right)^3 \nu^2 \, \overline{a}^2 \, \sigma_\ell^2 \, \delta(f)$$

$$\text{with } z = (2\pi\sigma_\ell f)^2. \tag{16}$$

The asymptotic behavior of spectrum (16) is [2, eq. 9.7.1]

$$G_I(f) \sim \frac{\nu \, \overline{a^2}}{(2\pi)^{3/2} \sigma_\ell} f^{-3} \quad \text{as} \quad f \to +\infty. \tag{17}$$

That is, the spectrum decays at a -30 dB/decade rate at large frequencies; this is due to the square root singularities at $x = \pm 1$ of pulse F given in (2). This decay rate has been observed in some spectral analyses of under-ice profiles, and was one of the reasons for choosing the specific circular pulse in (2) for this investigation.

The spectrum in (16) is plotted in figure 4, for the choice of parameters earlier in (10), as a dashed line, normalized to 0 dB at f = 0. Superposed is a linear-predictive spectral analysis result with predictive order 10, for the 8000 data points of figure 3C. The two results are in excellent agreement, even at the -50 dB level, with the inevitable 3 dB aliasing effect at the Nyquist frequency, as indicated.

The correlation $R_I(\tau)$ in (11) is evaluated in (A-23) through (A-33), for the example (2) and (4), with the result

$$R_I(\tau) = \frac{8}{3}(2\pi)^{1/2}\,\nu\,\overline{a^2}\,\sigma_\ell\;s\,\exp(-s)\,[(1+4s)\,K_1(s) - (3+4s)\,K_0(s)] +$$

$$+\left(\frac{\pi}{2}\right)^3 \nu^2\,\overline{a}^2\,\sigma_\ell^2, \quad \text{with } s = \left(\frac{\tau}{4\sigma_\ell}\right)^2 . \tag{18}$$

This quantity, exclusive of the I_{dc}^2 term, and normalized at the origin, is plotted in figure 5 as a dashed line, for delays (lags) τ up to 100. It is seen to decay monotonically to zero as τ increases, and reach its 1/e value at approximately $\tau = 30$.

The remaining solid curve on figure 5 is the normalized sample autocorrelation function of the 8000 data point sequence in figure 3C, where the sample mean was subtracted from the given data. The agreement with theoretical result (18) is excellent. The dotted horizontal lines at $\pm 2\sigma$ in figure 5 are the ±2 sigma values of the correlation estimate at delays where the true correlation is presumed zero; the details of this analysis are given in appendix B.

This procedure is duplicated in figure 6, where the correlation function estimate out to lag $\tau = 1000$ is plotted. The drifting of the estimate outside the $\pm 2\sigma$ limits (at $\tau = 470$ and 820) is consistent with an occasional excursion of a random variable outside its $\pm 2\sigma$ range. The correlation estimate (used for figures 5 and 6) at time separation k is

$$R_k = \frac{1}{N} \sum_{n=k+1}^{N} x_n \, x_{n-k} \quad \text{for } k \geq 0 , \qquad (19)$$

where $\{x_n\}_1^N$ is the available data in figure 3C, with its sample mean removed.

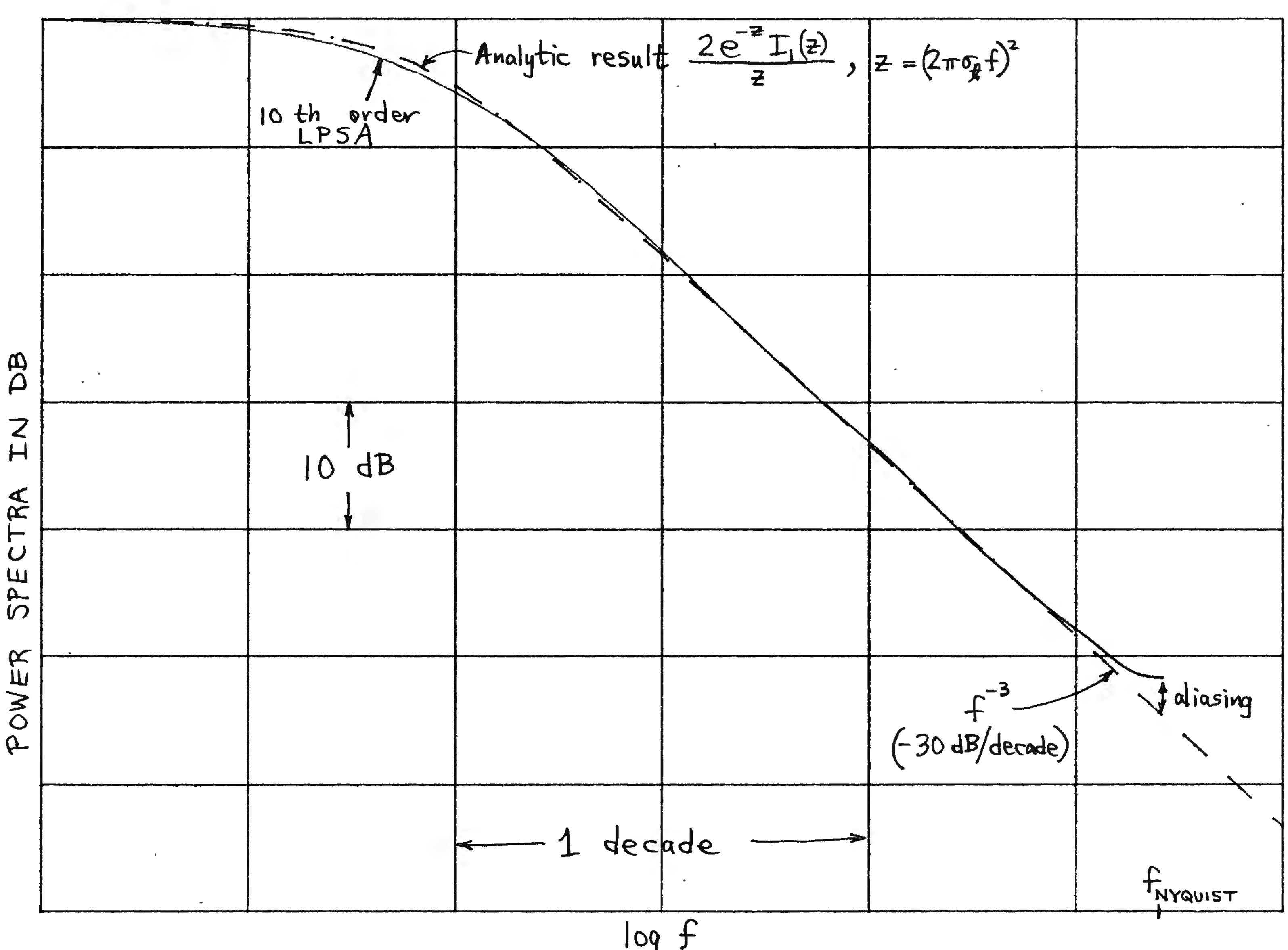

Figure 4. Comparison of Power Spectra

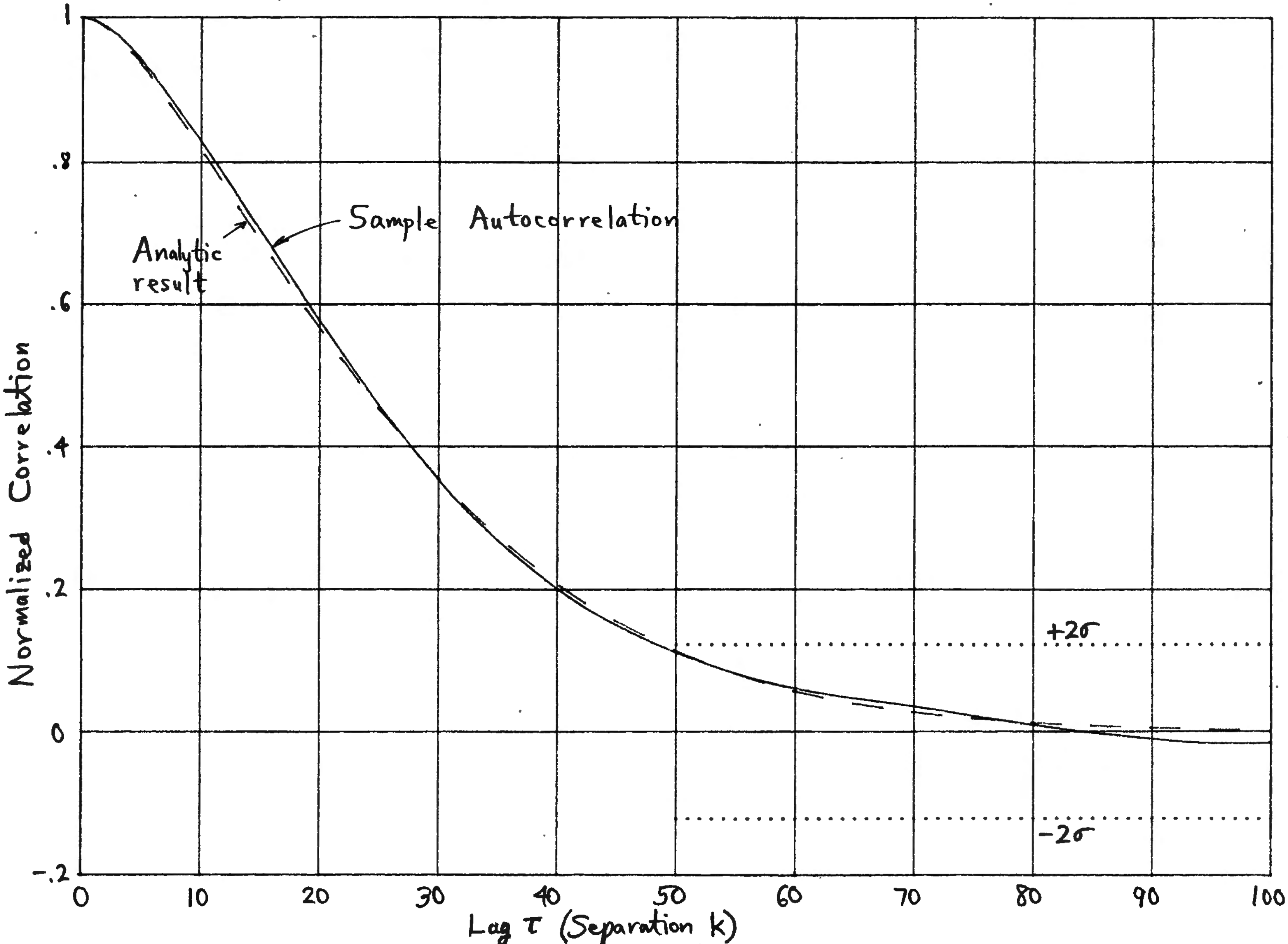

Figure 5. Estimate of Autocorrelation Function near origin

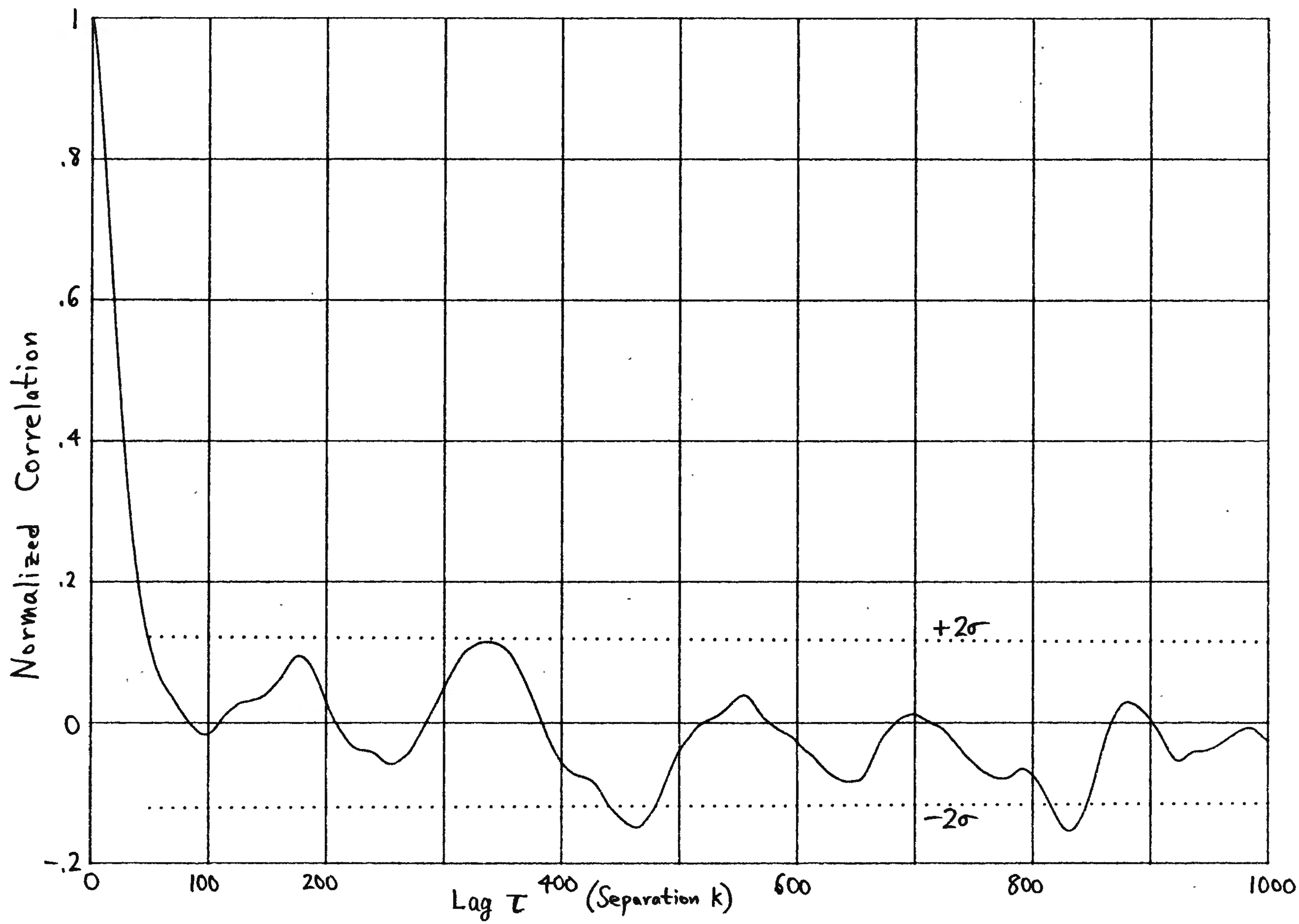

Figure 6. Estimate of Autocorrelation Function

TM No. 841208

AMPLITUDE STATISTICS OF SHOT NOISE

The first-order characteristic function of shot noise process I(t) is derived in appendix C; it is given by (C-9) as

$$f_I(\xi) = \exp\left[\nu\,\bar{\ell}\int dx\left\{f_a[\xi F(x)]-1\right\}\right] . \tag{20}$$

Here f_a is the first-order characteristic function of amplitude random variable a_k. Observe that the probability density function $p(\ell)$ of duration ℓ_k is irrelevant to characteristic function f_I, except for its mean $\bar{\ell}$; this is in contrast to the spectrum and correlation results in (11) and (14), where p(a) was irrelevant except for parameters $\bar{a}$ and $\overline{a^2}$. (For $\ell_k = 1$ for all k, (20) reduces to a simplified version of [1, eq. 1.5-4].)

The characteristic function of the amplitude random variable a_k can be expanded in terms of its moments

$$\mu_a(n) = \overline{a^n} = \int da\; a^n\, p(a) \quad \text{for } n \geq 0 , \tag{21}$$

according to

$$f_a(\xi) = \sum_{n=0}^{\infty} \mu_a(n)(i\xi)^n/n! \quad . \tag{22}$$

This result is useful if the ℓn of (20) is expanded in a series in ξ; namely

$$\ell n\; f_I(\xi) = \nu\,\bar{\ell}\sum_{n=1}^{\infty} \mu_a(n)(i\xi)^n \int dx\; F^n(x)/n! \quad , \tag{23}$$

giving immediately the cumulants of I(t) as

$$\chi_I(n) = \nu\,\bar{\ell}\,\mu_a(n)\int dx\; F^n(x) \quad \text{for } n \geq 1 . \tag{24}$$

That is, the n-th cumulant of I(t) is proportional to the n-th moment of random variable a_k as well as the n-th "moment" of pulse F. (For $\ell_k = 1$ for all k, (24) reduces to [1, eq. 1.5-2].)

The normalized cumulant of I(t) is

$$\gamma_I(n) = \frac{\chi_I(n)}{[\chi_I(2)]^{n/2}} = \frac{1}{(\nu\bar{\ell})^{\frac{n}{2}-1}} \frac{\mu_a(n) \int dx\ F^n(x)}{\left[\mu_a(2) \int dx\ F^2(x)\right]^{n/2}} . \qquad (25)$$

In particular, the coefficients of skewness and excess [3, pp. 184 and 187] are

$$\gamma_I(3) = \frac{1}{(\nu\bar{\ell})^{1/2}} \frac{\mu_a(3) \int dx\ F^3(x)}{\left[\mu_a(2) \int dx\ F^2(x)\right]^{3/2}} \qquad (26)$$

and

$$\gamma_I(4) = \frac{1}{\nu\bar{\ell}} \frac{\mu_a(4) \int dx\ F^4(x)}{\left[\mu_a(2) \int dx\ F^2(x)\right]^{2}} . \qquad (27)$$

These quantities are very important measures of the approach of I(t) to a Gaussian process; if $\nu\bar{\ell}$ is very large, the normalized cumulants $\gamma_I(n)$ are all substantially zero for $n \geq 3$, meaning that I(t) is nearly Gaussian. Thus although probability density function $p(\ell)$ is not directly relevant to the probability density function or characteristic function (20) of I(t), the exact probability density function of I(t) is critically dependent on the mean $\bar{\ell}$ through the dimensionless parameter $\nu\bar{\ell}$. More precisely, (26) and (27) are the critical quantities; see also [1, eq. 1.6-3].

If either the third moment of random variable a_k is zero, or if the third moment of pulse F is zero, then $\gamma_I(3) = 0$. In that case, $\gamma_I(4)$ is the most important statistic measuring the applicability of the central limit theorem; $\gamma_I(4)$ can never be zero for shot noise, since neither the fourth moment of random variable a_k or pulse F can be zero (except in a trivial case).

The first moment of shot noise I(t) is the mean

$$I_{dc} = \overline{I(t)} = \chi_I(1) = \nu \, \overline{\ell} \, \overline{a} \int dx \; F(x) \tag{28}$$

and has already been encountered in (12). It can be zero only if the first moment of random variable a_k or of pulse F is zero.

Example

Numerous cases have been considered in appendix C; in the main body here, we limit attention to example (2) and (3) presented earlier. We find

$$\mu_a(n) = 2^{\frac{n}{2}} \, \Gamma\!\left(\frac{n}{2} + 1\right) \sigma_a^n \quad \text{for } n \geq 0 \, ,$$

$$\int dx \; F^n(x) = \frac{2^{n+1} \, \Gamma^2\left(\frac{n}{2} + 1\right)}{\Gamma(n+2)} \quad \text{for } n \geq 0 \, . \tag{29}$$

Then (26) and (27) yield result (9) quoted earlier.

The realization of shot noise process I(t) in figure 3C employed the parameters in (10). The sample cumulative distribution function of these 8000 data points is depicted in figure 7, on a normal probability ordinate; thus a truly Gaussian random variable would have the straight line character indicated. The significant deviation of the sample cumulative distribution function from the Gaussian line is due to the small value of the overlap factor in (8), namely

$$\Gamma_k \, \nu = 2 \, \mathcal{I}_k \, \nu = 6.2 \; . \tag{30}$$

The moments in (29) are all positive and are easily numerically evaluated via recursion; hence the cumulants in (24) can be accurately evaluated for high-order n. When these cumulants are employed in a generalized Laguerre expansion of the cumulative distribution function of I(t), using 32 moments of (29), the solid curve in figure 8 is obtained. The sample cumulative distribution function of figure 7 is duplicated here, although the abscissa is scaled differently. The agreement between theory and experiment in figure 8 is excellent, considering the fact that we only have about 8000/30 = 270 effectively independent samples of I(t) in figure 3C; the denominator factor of 30 here is the effective correlation duration, previously identified in figure 5 at the 1/e point.

Finally, when the same 32 moments are used in a generalized Laguerre expansion of the probability density function of I(t), the result in figure 9 is obtained. The small bump near the origin is real and accurate; it and the non-symmetric tails of the probability density function confirm the distinctly non-Gaussian character of I(t). The method for the determination of the cumulative distribution function and probability density function in figures 8 and 9 will be presented in a NUSC Technical Report [4] by the author; the programs are listed here in appendix D, along with an example of the sequence of Laguerre coefficients.

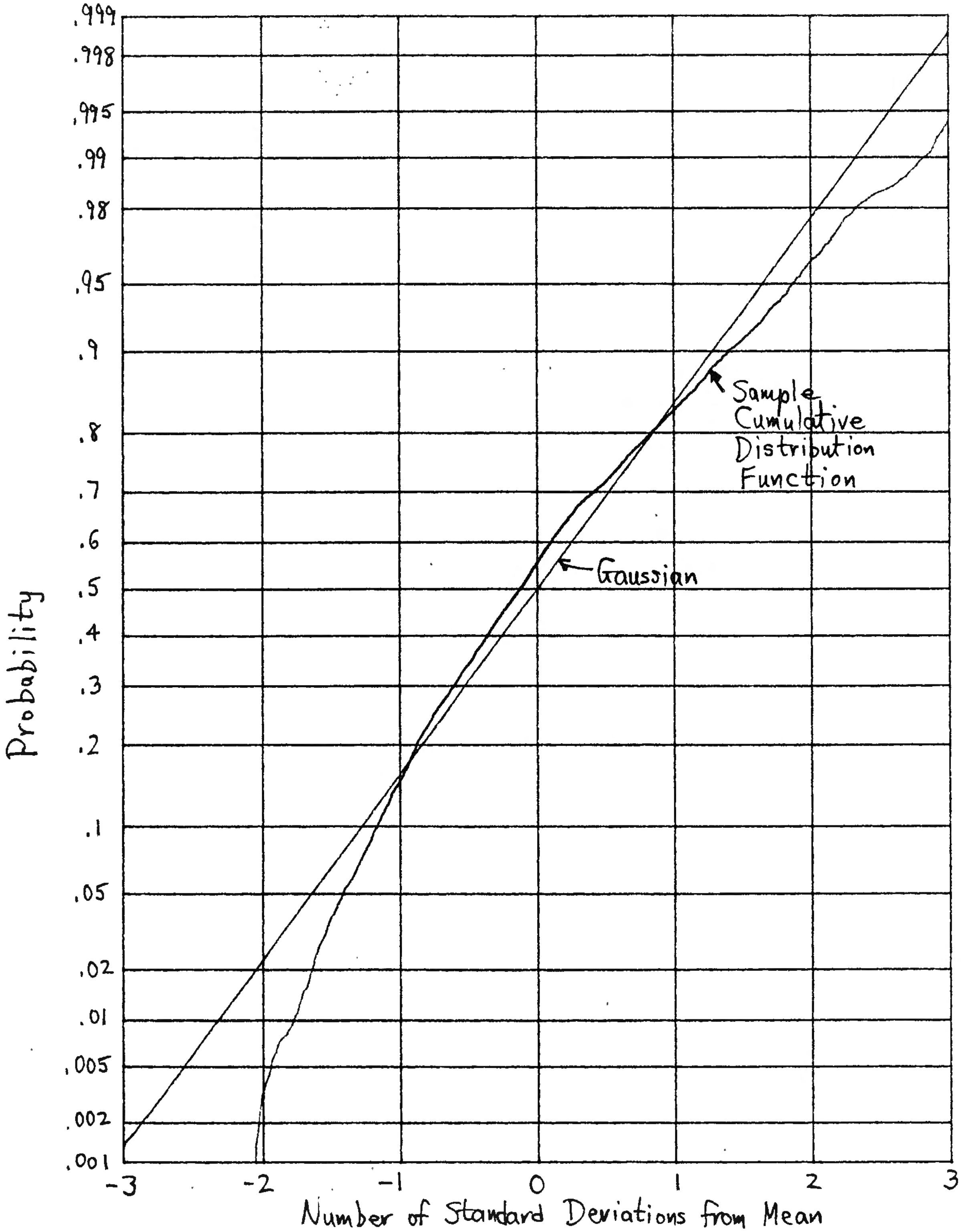

Figure 7. Estimate of Cumulative Distribution Function

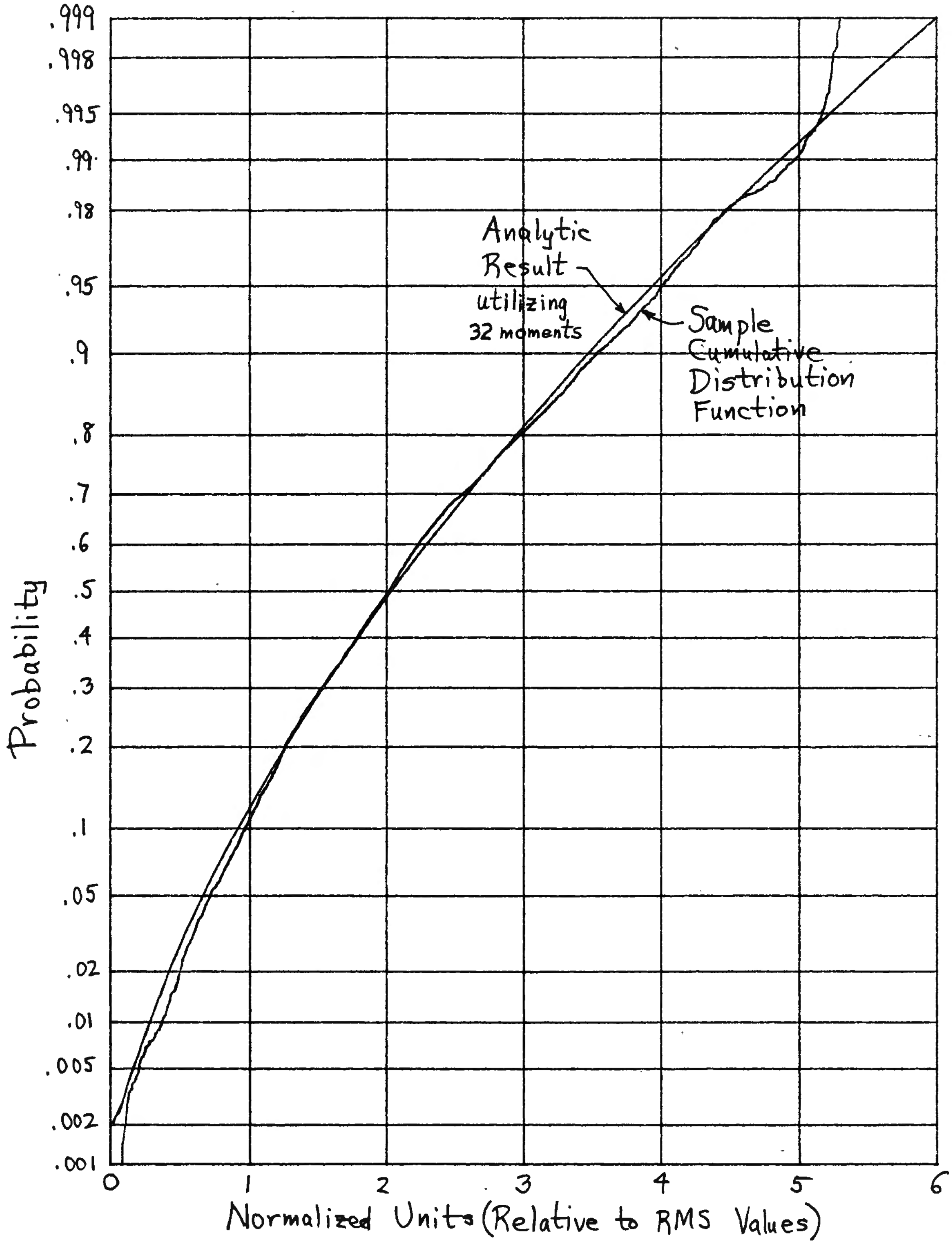

Figure 8. Comparison of Cumulative Distribution Functions

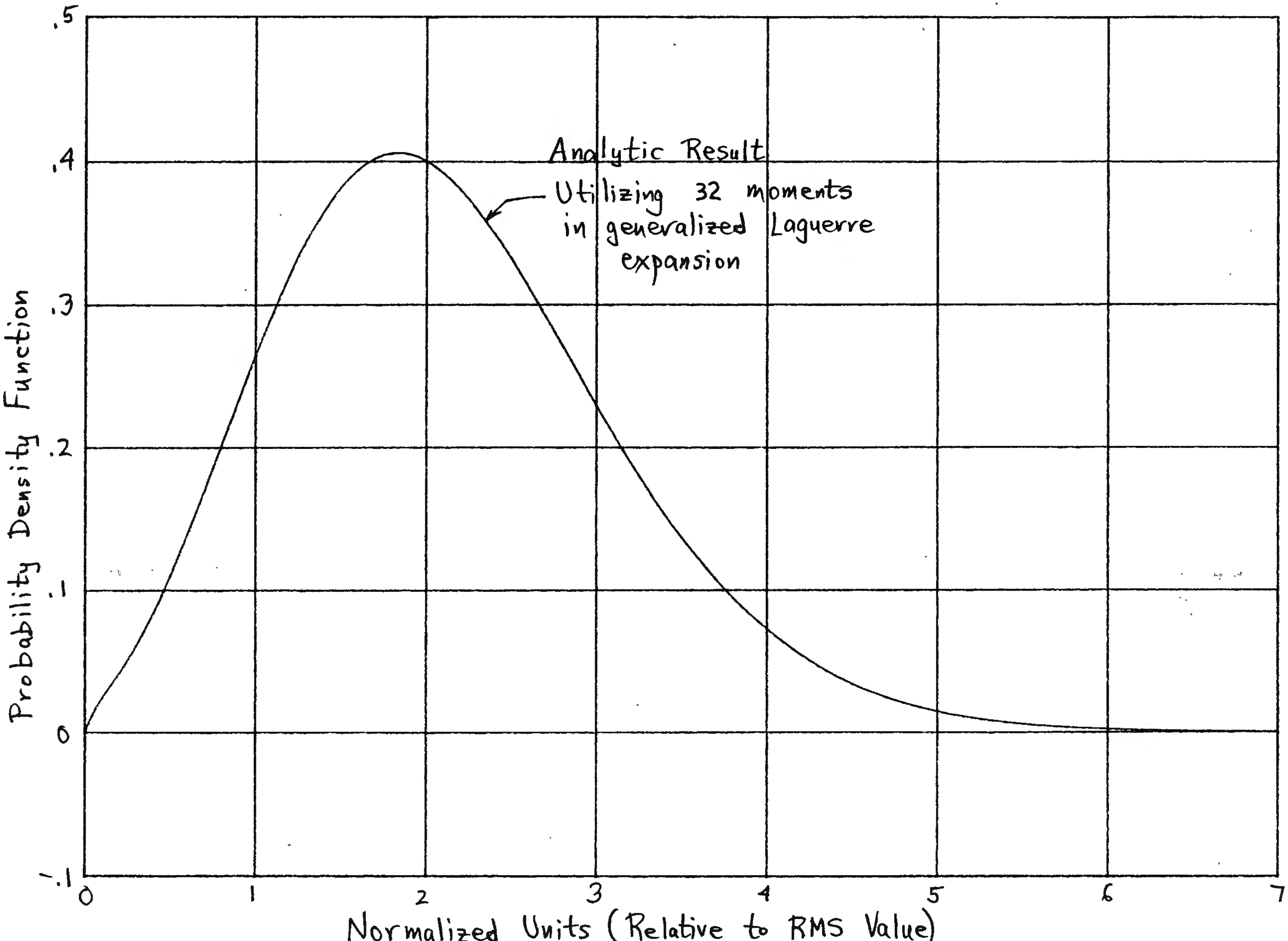

Figure 9. Theoretical Probability Density Function (Continuous Portion)

APPENDIX A. DERIVATION OF SPECTRUM AND CORRELATION

The method employed below follows that given by Rice [1, sections 1.4 and 1.5] rather closely. We generalize [1, eq. 1.3-1] to the current form introduced in (1):

$$I_K(t) = \sum_{k=1}^{K} a_k \; F\left(\frac{t-t_k}{\ell_k}\right) \quad , \tag{A-1}$$

where $\{a_k\}$, $\{t_k\}$, $\{\ell_k\}$ are all independent random variables. K is the presumed number of pulses to occur in a large time interval T, and a_k is a random amplitude as in [1, eq. 1.5-1]; but random duration ℓ_k is new. Then product

$$I_K(t)\; I_K(t-\tau) = \sum_{k=1}^{K} a_k^2 \; F\left(\frac{t-t_k}{\ell_k}\right) \; F\left(\frac{t-\tau-t_k}{\ell_k}\right) +$$

$$+ \sum_{k=1}^{K} \sum_{\substack{m=1 \\ k \neq m}}^{K} a_k \; a_m \; F\left(\frac{t-t_k}{\ell_k}\right) \; F\left(\frac{t-\tau-t_m}{\ell_m}\right) . \tag{A-2}$$

Holding random variables $\{a_k\}$ and $\{\ell_k\}$ fixed for now, the statistical average of (A-2) over $\{t_k\}$ is

$$\sum_{k=1}^{K} a_k^2 \; \frac{1}{T} \int_T dt_k \; F\left(\frac{t-t_k}{\ell_k}\right) \; F\left(\frac{t-\tau-t_k}{\ell_k}\right) +$$

$$+ \sum_{k=1}^{K} \sum_{\substack{m=1 \\ k \neq m}}^{K} a_k \; a_m \; \frac{1}{T} \int_T dt_k \; F\left(\frac{t-t_k}{\ell_k}\right) \frac{1}{T} \int_T dt_m \; F\left(\frac{t-\tau-t_m}{\ell_m}\right) =$$

$$\cong \frac{1}{T} \sum_{k=1}^{K} a_k^2 \; \ell_k \; \phi(\tau/\ell_k) + \frac{1}{T^2} \sum_{k=1}^{K} \sum_{\substack{m=1 \\ k \neq m}}^{K} a_k \; a_m \; \ell_k \; \ell_m \; S^2(0) \; , \tag{A-3}$$

where T is an arbitrary large (but finite) time interval, and

$$\phi(y) = \int dx \; F(x) \; F(x-y) \tag{A-4}$$

is the aperiodic autocorrelation of pulse F, while

$$S(f) = \int dx \; \exp(-i2\pi fx) \; F(x) \tag{A-5}$$

is the voltage density spectrum of F.

The remaining averages over independent random variables $\{a_k\}$ and $\{\ell_k\}$ in (A-3) now yield

$$\frac{1}{T} K \, \overline{a^2} \int d\ell \; p(\ell) \ell \; \phi(\tau/\ell) + \frac{1}{T^2} (K^2-K) \, [\bar{a} \, \bar{\ell} \; S(0)]^2, \tag{A-6}$$

where $p(\ell)$ is the probability density function of random variable ℓ_k.

Now K is itself a random variable, with discrete probability (in an interval T) of [1, eq. 1.1-3]

$$\frac{(\nu T)^K}{K!} \exp(-\nu T) \quad \text{for } K = 0, 1, 2, \ldots \, . \tag{A-7}$$

There then follows the characteristic function of random variable K as

$$f_K(\xi) = \exp\left(\nu T[\exp(i\xi) - 1]\right), \tag{A-8}$$

with series expansion

$$\ln f_K(\xi) = \nu T \, [\exp(i\xi)-1] = \nu T \sum_{n=1}^{\infty} (i\xi)^n/n! \; . \tag{A-9}$$

Thus the cumulants of random variable K are all equal,

$$\chi_K(n) = \nu T \quad \text{for } n \geq 1 \; , \tag{A-10}$$

giving in particular the first two moments

$$\overline{K} = \nu T, \; \overline{K^2} = \nu T(\nu T + 1) \; . \tag{A-11}$$

The use of (A-11), to perform the remaining average of (A-6) with respect to random variable K, then yields the correlation function of the shot noise process I(t):

$$R_I(\tau) = \nu\, \overline{a^2} \int d\ell\; p(\ell)\,\ell\; \phi(\tau/\ell) + [\nu\, \bar{a}\, \bar{\ell}\; S(0)]^2 . \qquad \text{(A-12)}$$

The dc component of I(t) is

$$I_{dc} = \nu\, \bar{a}\, \bar{\ell}\; S(0) = \nu\, \bar{a}\, \bar{\ell} \int dx\; F(x) . \qquad \text{(A-13)}$$

The spectrum of I(t) is the Fourier transform of (A-12):

$$G_I(f) = \nu\, \overline{a^2} \int d\ell\; p(\ell)\, \ell^2\, \Phi(\ell f) + I_{dc}^2\, \delta(f) , \qquad \text{(A-14)}$$

where

$$\Phi(f) = \int d\tau\, \exp(-i2\pi f\tau)\, \phi(\tau) =$$

$$= \int d\tau\, \exp(-i2\pi f\tau) \int dx\; F(x)\; F(x-\tau) = |S(f)|^2 , \qquad \text{(A-15)}$$

by use of (A-4) and (A-5). Thus (A-14) can be expressed as

$$G_I(f) = \nu\, \overline{a^2} \int d\ell\; p(\ell)\, \ell^2\; |S(\ell f)|^2 + I_{dc}^2\, \delta(f) . \qquad \text{(A-16)}$$

$|S(f)|^2$ is the energy density spectrum of pulse F.

Example

The example of interest here is given in (2) and (4):

$$F(x) = \left\{ \begin{matrix} (1-x^2)^{1/2} & \text{for} & |x| < 1 \\ 0 & \text{for} & |x| > 1 \end{matrix} \right\} ,$$

$$p(\ell) = \frac{\ell}{\sigma_\ell^2} \exp\left(\frac{-\ell^2}{2\sigma_\ell^2}\right) U(\ell) . \qquad \text{(A-17)}$$

Then from (A-5) and [5, eq. 3.752 2],

$$S(f) = \int_{-1}^{1} dx \exp(-i2\pi fx) \left(1-x^2\right)^{1/2} = \frac{J_1(2\pi f)}{2f} . \tag{A-18}$$

Substitution of (A-17) and (A-18) in the integral in (A-16) yields, by use of [5, eq. 6.633 2],

$$\int d\ell \frac{\ell}{\sigma_\ell^2} \exp\left(\frac{-\ell^2}{2\sigma_\ell^2}\right) \frac{J_1^2(2\pi f)}{4f^2} = 2\pi^2\sigma_\ell^2 \frac{2 \exp(-z) I_1(z)}{z} , \tag{A-19}$$

where

$$z = (2\pi\sigma_\ell f)^2. \tag{A-20}$$

Then the spectrum (A-16) is given by

$$G_I(f) = 2\pi^2 \nu \overline{a^2} \sigma_\ell^2 \frac{2 \exp(-z) I_1(z)}{z} + I_{dc}^2 \delta(f) , \tag{A-21}$$

where

$$I_{dc} = \nu \bar{a} \bar{\ell} S(0) = \left(\frac{\pi}{2}\right)^{3/2} \nu \bar{a} \sigma_\ell \tag{A-22}$$

by means of (A-13), (A-18), and (6).

To determine the correlation of shot noise process I(t), we consider first the continuous portion of the spectrum in (A-21):

$$G_c(f) = 2\pi^2 \nu \overline{a^2} \sigma_\ell^2 \frac{2 \exp(-4\pi^2\sigma_\ell^2 f^2) I_1(4\pi^2\sigma_\ell^2 f^2)}{4\pi^2\sigma_\ell^2 f^2} . \tag{A-23}$$

The corresponding correlation is

$$R_C(\tau) = \int_{-\infty}^{+\infty} df \; \exp(i2\pi f\tau)\; G_C(f) =$$

$$= 4\pi^2 \; \nu \; \overline{a^2} \; \sigma_\ell^2 \int_0^\infty df \; 2\cos(2\pi f\tau) \; \frac{\exp(-4\pi^2\sigma_\ell^2 f^2)\; I_1(4\pi^2\sigma_\ell^2 f^2)}{4\pi^2\sigma_\ell^2 f^2} =$$

$$= 2\pi \; \nu \; \overline{a^2} \; \sigma_\ell \int_0^\infty dz \; \cos\left(\frac{\tau}{\sigma_\ell} z^{1/2}\right) \frac{\exp(-z)\; I_1(z)}{z^{3/2}} =$$

$$= 2^{3/2} \pi \; \nu \; \overline{a^2} \; \sigma_\ell \; \exp(-s)\; W_{-\frac{3}{2},\frac{1}{2}}(2s) \;, \tag{A-24}$$

where we employed (A-20) and [5, eq. 6.755 2], and defined

$$s = \left(\frac{\tau}{4\sigma_\ell}\right)^2 . \tag{A-25}$$

The W-function in (A-24) is the Whittaker function [2, p. 505].

Now by [5, eqs. 9.232 1 and 9.222 1], we have

$$W_{-\frac{3}{2},\frac{1}{2}}(2s) = W_{-\frac{3}{2},-\frac{1}{2}}(2s) = \frac{\exp(-s)}{\Gamma(3/2)} \int_0^\infty dt \; \exp(-2st)\; t^{1/2} (1+t)^{-5/2} =$$

$$= \frac{2}{\pi^{1/2}} \exp(-s) \int_0^\infty dt \; \exp(-2st) \left[\frac{1}{t^{1/2}(1+t)^{3/2}} - \frac{1}{t^{1/2}(1+t)^{5/2}}\right] . \tag{A-26}$$

But according to [5, eq. 3.364 3],

$$\int_0^\infty dt \; \frac{\exp(-2st)}{t^{1/2}(a+t)^{1/2}} = \exp(as)\; K_0(as) \; . \tag{A-27}$$

Partial differention with respect to a then yields

$$-\frac{1}{2}\int_0^\infty dt\,\frac{\exp(-2st)}{t^{1/2}(a+t)^{3/2}} = s\,\exp(as)\,[K_0(as) - K_1(as)] \qquad \text{(A-28)}$$

and (repeated)

$$\frac{3}{4}\int_0^\infty dt\,\frac{\exp(-2st)}{t^{1/2}(a+t)^{5/2}} = s^2\,\exp(as)\left[2K_0(as) - 2K_1(as) + \frac{K_1(as)}{as}\right]. \qquad \text{(A-29)}$$

Here we used [2, eq. 9.6.28] in the forms

$$K_0'(z) = -K_1(z), \quad K_1'(z) = -K_0(z) - \frac{K_1(z)}{z}. \qquad \text{(A-30)}$$

If we now set a = 1 in (A-28) and (A-29), and then employ these results in (A-26), we obtain

$$W_{-\frac{3}{2},\frac{1}{2}}(2s) = \frac{2}{\pi^{1/2}}\frac{2}{3}s\left[(1+4s)K_1(s) - (3+4s)K_0(s)\right]. \qquad \text{(A-31)}$$

Finally, the use of (A-31) in (A-24) yields

$$R_c(\tau) = \frac{8}{3}(2\pi)^{1/2}\,\nu\,\overline{a^2}\,\sigma_\ell\,s\,\exp(-s)\left[(1+4s)K_1(s) - (3+4s)K_0(s)\right]. \qquad \text{(A-32)}$$

The Fourier transform of the impulsive part of the spectrum in (A-21) is simply the constant

$$I_{dc}^2 = \left(\frac{\pi}{2}\right)^3 \nu^2\,\overline{a}^2\,\sigma_\ell^2\,, \qquad \text{(A-33)}$$

which must be added to $R_c(\tau)$ in (A-32) to obtain $R_I(\tau)$. Here s is given by (A-25).

As $\tau \to 0+$, there follows from (A-32),

$$\lim_{\tau\to 0+} R_c(\tau) = \frac{8}{3}(2\pi)^{1/2}\,\nu\,\overline{a^2}\,\sigma_\ell\,. \qquad \text{(A-34)}$$

APPENDIX B. VARIANCE OF CORRELATION ESTIMATE

Let the available data be $\{x_n\}_1^N$, with zero mean and variance σ^2:

$$\overline{x_n} = 0, \quad \overline{x_n^2} = \sigma^2 \quad \text{for } 1 \leq n \leq N . \tag{B-1}$$

The autocorrelation estimate at delay k is defined here as

$$R_k = \frac{1}{N} \sum_{n=k+1}^{N} x_n \, x_{n-k} \quad \text{for } k \geq 0 . \tag{B-2}$$

At delay 0, the mean value of estimate R_o is

$$\overline{R_o} = \frac{1}{N} \sum_{n=1}^{N} \overline{x_n^2} = \sigma^2. \tag{B-3}$$

We now want to evaluate the standard deviation of estimate R_k at delays k large enough that x_n and x_{n-k} are statistically independent. We have mean value

$$\overline{R_k} = \frac{1}{N} \sum_{n=k+1}^{N} \overline{x_n} \, \overline{x_{n-k}} = 0 , \tag{B-4}$$

using the independence at separation k. The mean square value of estimate R_k is

$$\overline{R_k^2} = \frac{1}{N^2} \sum_{m,n=k+1}^{N} \overline{x_m \, x_n \, x_{m-k} \, x_{n-k}} \, . \tag{B-5}$$

For the large separation values k of interest here, the only statistical dependence that contributes non-trivially to the double sum is the following:

$$\overline{R_k^2} = \frac{1}{N^2} \sum_{m,n=k+1}^{N} \overline{x_m\, x_n}\; \overline{x_{m-k}\, x_{n-k}} = \frac{\sigma^4}{N^2} \sum_{m,n=k+1}^{N} \rho^2(m-n) =$$

$$= \frac{\sigma^4}{N^2} \sum_{|n|<N-k} (N-k-|n|)\, \rho^2(n) \cong \frac{\sigma^4}{N^2} (N-k) \sum_n \rho^2(n) \; . \qquad \text{(B-6)}$$

Here ρ is the correlation coefficient of data $\{x_n\}$, and we have assumed that N is moderately larger than the effective correlation length of ρ. The ratio of the standard deviation of estimate R_k to the mean value at k=0 is then the normalized standard deviation at separation k:

$$\sigma_k' \cong \frac{1}{N}\left[(N-k) \sum_n \rho^2(n)\right]^{1/2} . \qquad \text{(B-7)}$$

Notice that <u>no</u> Gaussian assumptions on data $\{x_n\}_1^N$ have been employed in this analysis; however, $\rho(k)$ is essentially zero at the k values of interest.

As an example, for an exponential correlation of effective length K_e, there follows

$$\sum_n \rho^2(n) = \sum_n \exp\left(-2\frac{|n|}{K_e}\right) \cong \int dx\, \exp\left(-2\frac{|x|}{K_e}\right) = K_e \; , \qquad \text{(B-8)}$$

where we assume that K_e is moderately larger than unity. Then (B-7) yields

$$\sigma_k' \cong \frac{1}{N}[(N-k)K_e]^{1/2} . \qquad \text{(B-9)}$$

These results hold only for those values of k where $\rho(k)$ has substantially gone to zero. Larger values of K_e lead to larger relative standard deviations; this is consistent with the fact that there are then a lesser number of effectively-independent samples in the limited data set of length N.

For the 8000 data point example of interest here, inspection of figure 5 reveals that $K_e \cong 30$. Thus

$$\pm 2\sigma_k' = \pm \frac{(8000-k)^{1/2}}{730} . \tag{B-10}$$

These confidence limits are superposed as dotted lines on figures 5 and 6.

APPENDIX C. PROPERTIES OF CHARACTERISTIC FUNCTION OF SHOT NOISE

Derivation of Characteristic Function

The method of derivation of the characteristic function of I(t) presented here parallels that of Rice [1, sections 1.4 and 1.5] very closely. We generalize [1, eq. 1.3-1] to

$$I_K(t) = \sum_{k=1}^{K} a_k \, F\left(\frac{t-t_k}{\ell_k}\right) \tag{C-1}$$

where $\{a_k\}$, $\{t_k\}$, $\{\ell_k\}$ are all independent random variables; see (A-1) and the ensuing discussion. The characteristic function of an individual component in (C-1) is

$$f_1(\xi) = \overline{\exp\left[i\xi a_k \, F\left(\frac{t-t_k}{\ell_k}\right)\right]} \;, \tag{C-2}$$

where the statistical average is over a_k , t_k , ℓ_k . The average over t_k (for fixed a_k, ℓ_k) is, for T a large but finite time interval [1, p. 152],

$$\frac{1}{T}\int_0^T dt_k \, \exp\left[i\xi a_k \, F\left(\frac{t-t_k}{\ell_k}\right)\right] =$$

$$= \frac{1}{T}\int_0^T dt_k \left\{\exp\left[i\xi a_k \, F\left(\frac{t-t_k}{\ell_k}\right)\right] - 1\right\} + 1 =$$

$$\cong \frac{1}{T}\int d\tau \left\{\exp\left[i\xi a_k \, F\left(\frac{t-\tau}{\ell_k}\right)\right] - 1\right\} + 1 \;, \tag{C-3}$$

for large T, where we have used the fact that

$$F(x) \rightarrow 0 \text{ as } x \rightarrow \pm\infty . \qquad \text{(C-4)}$$

Let $x = (t-\tau_k)/\ell_k$ in (C-3) to get

$$\frac{1}{T}\ell_k \int dx\left\{\exp[i\xi a_k F(x)]-1\right\} + 1 . \qquad \text{(C-5)}$$

Now performing the averages on random variables ℓ_k and a_k, we have, for the characteristic function of an individual component of (C-1),

$$f_1(\xi) = \frac{1}{T}\bar{\ell}\int da\ p(a)\int dx\left\{\exp[i\xi a\ F(x)]-1\right\} + 1 , \qquad \text{(C-6)}$$

where p(a) is the probability density function of random variable a_k.

Interchanging integrals, (C-6) becomes

$$f_1(\xi) = \frac{1}{T}\bar{\ell}\int dx\left\{f_a[\xi F(x)]-1\right\} + 1 , \qquad \text{(C-7)}$$

where f_a is the characteristic function of amplitude a_k. Then from (C-1), since all the individual random variables are independent, the characteristic function of $I_K(t)$ is

$$f_{I_K}(\xi) = [f_1(\xi)]^K . \qquad \text{(C-8)}$$

Finally, the characteristic function of total shot noise process (1) is, by use of discrete probability distribution (A-7) for random variable K, given by the average

$$f_I(\xi) = \sum_{K=0}^{\infty} \frac{(\nu T)^K}{K!} \exp(-\nu T)\, f_{I_K}(\xi) =$$

$$= \exp[-\nu T + \nu T\, f_1(\xi)] =$$

$$= \exp[\nu \overline{\ell} \int dx \{f_a[\xi F(x)] - 1\}] \; . \qquad \text{(C-9)}$$

The (imprecise) large time interval T has dropped out of the general result (C-9). Also, the only parameter required about the duration random variable ℓ_k is its mean. The exact characteristic function f_a of amplitude a_k and the exact pulse shape F directly affect the characteristic function of I(t). For $\ell_k = 1$ for all k, (C-9) reduces to a simplified version of [1, eq. 1.5-4].

Cumulants of I(t)

The characteristic function of random amplitude a_k can be expanded in a power series

$$f_a(\xi) = \sum_{n=0}^{\infty} \mu_a(n) \frac{(i\xi)^n}{n!} \; , \qquad \text{(C-10)}$$

where $\mu_a(n)$ is the n-th moment of a_k:

$$\mu_a(n) = \overline{a^n} = \int da\, a^n\, p(a) \; . \qquad \text{(C-11)}$$

Then from (C-9), we develop

$$\ln f_I(\xi) = \nu \bar{\ell} \int dx \left\{ f_a[\xi F(x)] - 1 \right\} =$$

$$= \nu \bar{\ell} \sum_{n=1}^{\infty} \mu_a(n) \frac{(i\xi)^n}{n!} \int dx\ F^n(x) \ , \tag{C-12}$$

allowing for immediate identification of the cumulants of I(t) as

$$\chi_I(n) = \nu \bar{\ell}\ \mu_a(n) \int dx\ F^n(x) \quad \text{for } n \geq 1;\ \chi_I(0) = 0\ . \tag{C-13}$$

For $\ell_k = 1$ for all k, this reduces to [1, eq. 1.5-2].

The normalized cumulants of I(t) are

$$\gamma_I(n) = \frac{\chi_I(n)}{[\chi_I(2)]^{n/2}} = \frac{1}{(\nu\bar{\ell})^{\frac{n}{2}-1}} \frac{\mu_a(n) \int dx\ F^n(x)}{\left[\mu_a(2) \int dx\ F^2(x)\right]^{\frac{n}{2}}}\ . \tag{C-14}$$

These quantities tend to zero rapidly for $\nu\bar{\ell} \gg 1$; see also [1, eq. 1.6-3]. Thus $\nu\bar{\ell}$ has a pronounced effect on how Gaussian I(t) is.

Behavior of characteristic function $f_I(\xi)$ at $\xi = \pm\infty$

If pulse F(x) is non-zero only over (x_1, x_2), we have

$$\int dx \left\{ f_a[\xi F(x)] - 1 \right\} = \int_{x_1}^{x_2} dx \left\{ f_a[\xi F(x)] - 1 \right\}\ . \tag{C-15}$$

Now if random variable a_k has a characteristic function f_a with the property that

$$f_a(\pm\infty) = 0\ , \tag{C-16}$$

then

$$\text{(C-15)} \rightarrow \int_{x_1}^{x_2} dx \left\{0-1\right\} = -(x_2 - x_1) \text{ as } \xi \rightarrow \pm\infty, \qquad \text{(C-17)}$$

in which case (C-9) yields

$$f_I(\pm\infty) = \exp[-\nu\bar{\ell}(x_2 - x_1)] \; . \qquad \text{(C-18)}$$

If pulse extent $x_2 - x_1$ is infinite, as for the Gaussian or exponential pulses,

$$F(x) = \exp(-x^2) \text{ or } \exp(-x)U(x) \; , \qquad \text{(C-19)}$$

then (C-18) is zero. On the other hand, if $x_2 - x_1$ is finite, as for circular pulse

$$F(x) = \left\{ \begin{matrix} (1-x^2)^{1/2} \text{ for } |x| < 1 \\ 0 \quad \text{for } |x| > 1 \end{matrix} \right\}, \qquad \text{(C-20)}$$

then

$$f_I(\pm\infty) = \exp[-\nu\bar{\ell}2] > 0 \quad \text{for circular pulse.} \qquad \text{(C-21)}$$

This non-zero characteristic function value corresponds to an impulse at the origin of probability density function p_I, with area (C-21). Physically, this means that there are occasionally regions of the t-scale where <u>no</u> pulses overlap, and there $I(t) = 0$. The probability of this happening is, generally,

$$P_0 = \text{Prob}\left\{I(t) = 0\right\} = f_I(\pm\infty) = \exp[-\nu\bar{\ell}(x_2 - x_1)] \; . \qquad \text{(C-22)}$$

On the other hand, for the Gaussian or exponential pulses cited in (C-19), $x_2 - x_1 = +\infty$, and $f_I(\pm\infty) = 0$, meaning that there is no impulse at the origin of probability density function p_I. Physically, the infinite tails (even if single-sided, as for the exponential pulse) disallow I(t) ever from becoming zero.

Cumulants of Continuous Portion of p_I.

The impulse at the origin means that probability density function p_I and cumulative distribution function P_I can be expressed respectively as

$$p_I(u) = P_0 \, \delta(u) + p_c(u) ,$$

$$P_I(u) = P_0 + \int_0^u dt \; p_c(t) \quad \text{for } u > 0, \tag{C-23}$$

where $p_c(u)$ is a continuous function of u, with area $1-P_0$. The characteristic function relation corresponding to (C-23) is

$$f_I(\xi) = P_0 + f_c(\xi) , \tag{C-24}$$

and the moments are related according to

$$\mu_c(n) = \begin{cases} \mu_I(0) - P_0 & \text{for } n=0 \\ \mu_I(n) & \text{for } n \geq 1 \end{cases} . \tag{C-25}$$

The cumulants of f_c or p_c can then be found from these moments (C-25), by recursive relations; see [4] or [6]. This procedure is necessary to get accurate series expansions for the probability density function p_c and its cumulative distribution function, without having to approximate a delta function.

Overlap Factor

In the case where pulse extent $x_2 - x_1$ is finite, it is possible to find the average number of overlapping pulses at any one time instant; this statistic, denoted by $\overline{K_1}$, is called the overlap factor. In order to determine it in a simple fashion, we concoct a very special shot noise process: let

$$a_k = 1 \quad \text{for all } k \text{ ,}$$

$$F(x) = 1 \quad \text{for } x_1 < x < x_2 \text{ .} \tag{C-26}$$

Then I(t) is a step function with amplitudes limited to the values 0, 1, 2, ... Then obviously, the average number of overlapping pulses at one time instant is just

$$\overline{K_1} = \overline{I(t)} = \nu \overline{\ell}\, \mu_a(1) \int dx\ F(x) = \nu \overline{\ell}(x_2 - x_1) \text{ ,} \tag{C-27}$$

upon use of (C-13) with n=1 and (C-26). If we let

$$\overline{L} = \overline{\ell}(x_2 - x_1) \tag{C-28}$$

denote the average pulse duration, we have the overlap factor in the form

$$\overline{K_1} = \nu\, \overline{L} \text{ .} \tag{C-29}$$

For the Gaussian or exponential pulses in (C-19), we have $x_2 - x_1 = +\infty$, giving $\overline{L} = +\infty$, $\overline{K_1} = +\infty$. This is in fact true, since all the infinite tails overlap; however, it is not then an informative statistic.

Closed Form Characteristic Function Examples

There are a couple of examples of the circular pulse shape F and amplitude characteristic function f_a, where (C-9) can be evaluated in closed form. This furnishes an alternative to the moment approach [4] used here.

Consider the circular pulse in (C-20); then the integral in (C-9) is (using (C-15))

$$\int_{-1}^{1} dx \left\{ f_a\left[\xi\left(1-x^2\right)^{1/2}\right] - 1 \right\} = 2\int_0^{\frac{\pi}{2}} d\theta \cos\theta \, f_a[\xi \cos\theta] - 2 \; , \qquad \text{(C-30)}$$

which holds for any characteristic function f_a. Now first let the probability density function of a_k be exponential:

$$p(a) = \frac{1}{\mu_a} \exp\left(\frac{-a}{\mu_a}\right) U(a) \; , \quad f_a(\xi) = (1 - i\xi\mu_a)^{-1} \; . \qquad \text{(C-31)}$$

Substitution in (C-30) yields

$$2\int_0^{\frac{\pi}{2}} \frac{d\theta \cos\theta}{1-i\xi\mu_a \cos\theta} - 2 \; . \qquad \text{(C-32)}$$

But we know that

$$2\int_0^{\frac{\pi}{2}} \frac{d\theta \cos\theta}{1-z \cos\theta} = -\frac{\pi}{z} + \frac{4}{z\left(1-z^2\right)^{1/2}} \arctan\left[\left(\frac{1+z}{1-z}\right)^{1/2}\right] =$$

$$= -\frac{\pi}{z} + \frac{2}{z\left(1-z^2\right)^{1/2}} \arccos(-z) \; , \qquad \text{(C-33)}$$

via [5, eqs. 2.554 2 and 2.553 3]. Then letting $z = i\xi\mu_a$ and using [2, eqs. 4.4.2 with 4.4.26], (C-32) becomes

$$\frac{-2\,\ell n(s-\mu_a\xi) + i\pi(s-1)}{\mu_a \xi s} - 2, \quad \text{with } s = \left(1 + \mu_a^2 \xi^2\right)^{1/2}. \tag{C-34}$$

Combining these results in (C-9), the closed form characteristic function is

$$f_I(\xi) = \exp\left[-\frac{2\nu\bar{\ell}}{\mu_a \xi s}\left\{\mu_a \xi s + \ell n(s-\mu_a\xi) - i\,\frac{\pi}{2}(s-1)\right\}\right], \tag{C-35}$$

which holds for a circular pulse F and an exponential probability density function p(a).

The second example is the one considered in detail here, namely the Rayleigh probability density function p(a) given in (3). First substituting (C-30) in (C-9), we have characteristic function

$$f_I(\xi) = \exp[2\nu\bar{\ell}(J(\xi)-1)] , \tag{C-36}$$

where integral $J(\xi)$ is defined as

$$J(\xi) = \int_0^{\frac{\pi}{2}} d\theta \cos\theta \; f_a[\xi \cos\theta] . \tag{C-37}$$

For Rayleigh probability density function (3), (C-37) can be expressed as follows:

$$J(\xi) = \int_0^{\frac{\pi}{2}} d\theta \cos\theta \int_0^{\infty} da \exp(ia\xi\cos\theta)\,\frac{a}{\sigma_a^2}\exp\left(\frac{-a^2}{2\sigma_a^2}\right). \tag{C-38}$$

Transform to rectangular coordinates according to $a \cos\theta = \sigma_a x$, $a \sin\theta = \sigma_a y$, and obtain

$$J(\xi) = \iint_0^{\infty} dx\, dy\, \frac{x}{(x^2+y^2)^{1/2}} \exp\left(i\xi\sigma_a x - \frac{x^2+y^2}{2}\right). \tag{C-39}$$

But the integral on y here is, via $y = x\,u^{1/2}$, equal to

$$\frac{1}{2}\int_0^\infty \frac{du}{u^{1/2}(1+u)^{1/2}}\exp\left(-\frac{1}{2}x^2u\right) = \frac{1}{2}\exp\left(\frac{x^2}{4}\right)K_0\left(\frac{x^2}{4}\right), \tag{C-40}$$

the latter by means of [5, eq. 3.364 3]. Thus (C-39) becomes

$$J(\xi) = \int_0^\infty dx\; x\exp\left(i\xi\sigma_a x - \frac{x^2}{2}\right)\frac{1}{2}\exp\left(\frac{x^2}{4}\right)K_0\left(\frac{x^2}{4}\right) =$$

$$= \int_0^\infty du\,\exp(i\,2^{1/2}\sigma_a\xi\,u)\;u\,\exp\left(-\frac{u^2}{2}\right)K_0\left(\frac{u^2}{2}\right). \tag{C-41}$$

At this point, we have two alternatives. First, (C-41) could be efficiently evaluated for all ξ via an FFT; the decay of the integrand is according to $\exp(-u^2)$ for large u. Secondly, $J(\xi)$ can be expressed in a closed form in terms of a hypergeometric function; specifically

$$J(\xi) = {}_2F_2\left(1,\,1;\,\frac{1}{2},\,\frac{3}{2};\,-2b^2\right) +$$

$$+\; i\left(\frac{\pi}{2}\right)^{3/2} b\,\exp(-b^2)\,[I_0(b^2) - I_1(b^2)]\,, \tag{C-42}$$

where $b = \sigma_a\xi/2$. The upper line follows from [5, eq. 6.755 6], while the lower line used [5, eq. 6.755 9] with an application of partial derivative $\partial/\partial a$ to both sides. The characteristic function f_I is finally obtained by employing (C-42) in (C-36).

Still another alternative is afforded by use of the closed form for the characteristic function of the Rayleigh probability density function, as given in [7, eq. 6].

Moments for Some Particular Pulse Shapes F

The moments of pulse shape F were encountered in evaluating the cumulants $\chi_I(n)$ of shot noise I(t), according to (24) or (C-13) as

$$\mu_F(n) = \int dx\, F^n(x) \quad \text{for } n \geq 0 . \tag{C-43}$$

For circular pulse (C-20), [5, eq. 3.621 1] yields moments

$$\mu_F(n) = \int_{-1}^{1} dx\, (1-x^2)^{n/2} = 2\int_0^{\frac{\pi}{2}} d\theta\, (\cos\theta)^{n+1} = \frac{2^{n+1}\Gamma^2\left(\frac{n}{2}+1\right)}{\Gamma(n+2)} , \tag{C-44}$$

a result already quoted in (29).

More generally, for

$$F(x) = \begin{Bmatrix} (1-x^2)^\alpha & \text{for } |x| < 1 \\ 0 & \text{for } |x| > 1 \end{Bmatrix} , \tag{C-45}$$

[5, eq. 3.621 1] yields, with a trigonometric substitution,

$$\mu_F(n) = 2^{2n\alpha+1}\frac{\Gamma^2(n\alpha+1)}{\Gamma(2n\alpha+2)} . \tag{C-46}$$

For

$$F(x) = \begin{Bmatrix} (\cos x)^\alpha & \text{for } |x| < \frac{\pi}{2} \\ 0 & \text{for } |x| > \frac{\pi}{2} \end{Bmatrix} , \tag{C-47}$$

[5, eq. 3.621 1] yields directly

$$\mu_F(n) = 2^{n\alpha}\frac{\Gamma^2\left(\frac{n\alpha+1}{2}\right)}{\Gamma(n\alpha+1)} . \tag{C-48}$$

For

$$F(x) = x^{\alpha} \exp(-x) \, U(x) ,$$

$$\mu_F(n) = \frac{\Gamma(n\alpha+1)}{n^{n\alpha+1}} , \tag{C-49}$$

while for

$$F(x) = x^{\alpha} \exp(-x^2/2) \, U(x) ,$$

$$\mu_F(n) = \frac{2^{\frac{n\alpha-1}{2}} \Gamma\left(\frac{n\alpha+1}{2}\right)}{n^{\frac{n\alpha+1}{2}}} . \tag{C-50}$$

Both relations follow directly from the definition of the Γ function.

Some Probability Density Functions for Amplitude a_k

For probability density function

$$p(a) = \frac{(a/\alpha)^{\gamma} \exp(-a/\alpha)}{\alpha \Gamma(\gamma+1)} U(a) , \tag{C-51}$$

we have characteristic function

$$f_a(\xi) = (1-i\xi\alpha)^{-\gamma-1} \tag{C-52}$$

with moments

$$\mu_a(n) = (\gamma+1)_n \, \alpha^n \quad \text{for } n \geq 0 \tag{C-53}$$

and cumulants

$$\chi_a(n) = (n-1)! \, (\gamma+1) \, \alpha^n \quad \text{for } n \geq 1 . \tag{C-54}$$

This example subsumes the exponential probability density function, upon setting $\gamma = 0$.

For probability density function

$$p(a) = \frac{2(a/\alpha)^{\gamma} \exp(-a^2/\alpha^2)}{\alpha \Gamma\left(\frac{\gamma+1}{2}\right)} U(a) , \qquad \text{(C-55)}$$

we have moments

$$\mu_a(n) = \frac{\Gamma\left(\frac{n+\gamma+1}{2}\right)}{\Gamma\left(\frac{\gamma+1}{2}\right)} \alpha^n \quad \text{for } n \geq 0 . \qquad \text{(C-56)}$$

This example subsumes respectively the one-sided Gaussian for $\gamma=0$, the Rayleigh for $\gamma=1$, and the Maxwell probability density functions for $\gamma=2$. The result in (29) follows immediately by setting $\gamma=1$, $\alpha= 2^{1/2}\sigma_a$.

Convergence of Series for $\ell n\ f_I(\xi)$

A power series expansion for $\ell n\ f_I(\xi)$ was developed in (C-12), namely,

$$\ell n\ f_I(\xi) = \nu\bar{\lambda} \sum_{n=1}^{\infty} \mu_a(n)\ \mu_F(n)\ \frac{(i\xi)^n}{n!} ; \qquad \text{(C-57)}$$

here we employed (C-43). Since the moments in (C-57) can be easily evaluated via recursion, according to results in the above two subsections, it might be thought that (C-57) could be employed to evaluate the characteristic function of I(t) directly, without recourse to the more difficult approaches required in (C-9) or (C-35) or (C-36)-(C-42).

To see the drawbacks of this approach, consider first a circular pulse F and a generalized exponential probability density function p(a) as in (C-51); then a combination of (C-44) and (C-53) yields, for the n-th term of the sum in (C-57),

$$T_n = \frac{2(\gamma+1)_n \Gamma^2\left(\frac{n}{2}+1\right)}{n!\,(n+1)!} (i\xi\alpha 2)^n . \tag{C-58}$$

Then ratio

$$\frac{T_n}{T_{n-2}} = -\frac{(n+\gamma)(n+\gamma-1)}{n^2-1}\xi^2\alpha^2 \sim -\xi^2\alpha^2 \quad \text{as } n \to +\infty, \tag{C-59}$$

regardless of the value of γ. Therefore

$$\left|\frac{T_n}{T_{n-1}}\right| \sim |\xi|\alpha \quad \text{as } n \to +\infty, \tag{C-60}$$

meaning that series (C-57) only converges for $|\xi| < 1/\alpha$. So (C-57) is not a viable approach for the calculation of the characteristic function in this case.

As a second example, we consider the circular pulse F with the generalized Rayleigh probability density function in (C-55). Combination of (C-44) with (C-56) yields for the n-th term of series (C-57),

$$T_n = \frac{2\Gamma^2\left(\frac{n}{2}+1\right)\,\Gamma\left(\frac{n+\gamma+1}{2}\right)}{n!\,(n+1)!\,\Gamma\left(\frac{\gamma+1}{2}\right)} (i\xi\alpha 2)^n . \tag{C-61}$$

Then ratio

$$\frac{T_n}{T_{n-2}} = -\frac{n+\gamma-1}{n^2-1}\,\frac{\xi^2\alpha^2}{2} \sim -\frac{\xi^2\alpha^2}{2n} \quad \text{as } n \to +\infty, \tag{C-62}$$

regardless of γ. Therefore

$$\left|\frac{T_n}{T_{n-1}}\right| \sim \frac{|\xi|\alpha}{(2n)^{1/2}} \quad \text{as } n \to +\infty, \tag{C-63}$$

meaning that series (C-57) converges for all ξ. However, direct numerical evaluation of (C-57) via (C-61) and (C-62) loses all its significant digits for large ξ, long before $\ell n\ f_I(\xi)$ reaches its final value of $-2\bar{\ell}\nu + i0$, due to the alternating character of the series. So (C-57) is not a useful approach for evaluation of the characteristic function, except for small ξ. By contrast, the series expansion technique employed in [4] uses the moments to directly estimate the desired probability density function and cumulative distribution function of interest, for large arguments as well as small.

APPENDIX D. PROGRAMS FOR CUMULATIVE DISTRIBUTION FUNCTION AND PROBABILITY DENSITY FUNCTION

The programs used here to evaluate the cumulative distribution function and probability density function of shot noise are listed below. The n-th coefficient in a generalized Laguerre expansion of orthonormal polynomials is denoted by b_n and is plotted in figure D-1 for n = 0(1)70. It is seen to oscillate and decay with n until n = 32, at which point round-off error becomes important; however, by this time, $|b_n|$ has decayed below the 1E-5 level. The round-off error is so dominant beyond n = 35, that no useful results for b_n can be obtained then. The particular parameter values (α, β) used for the Laguerre weighting are indicated in the listings.

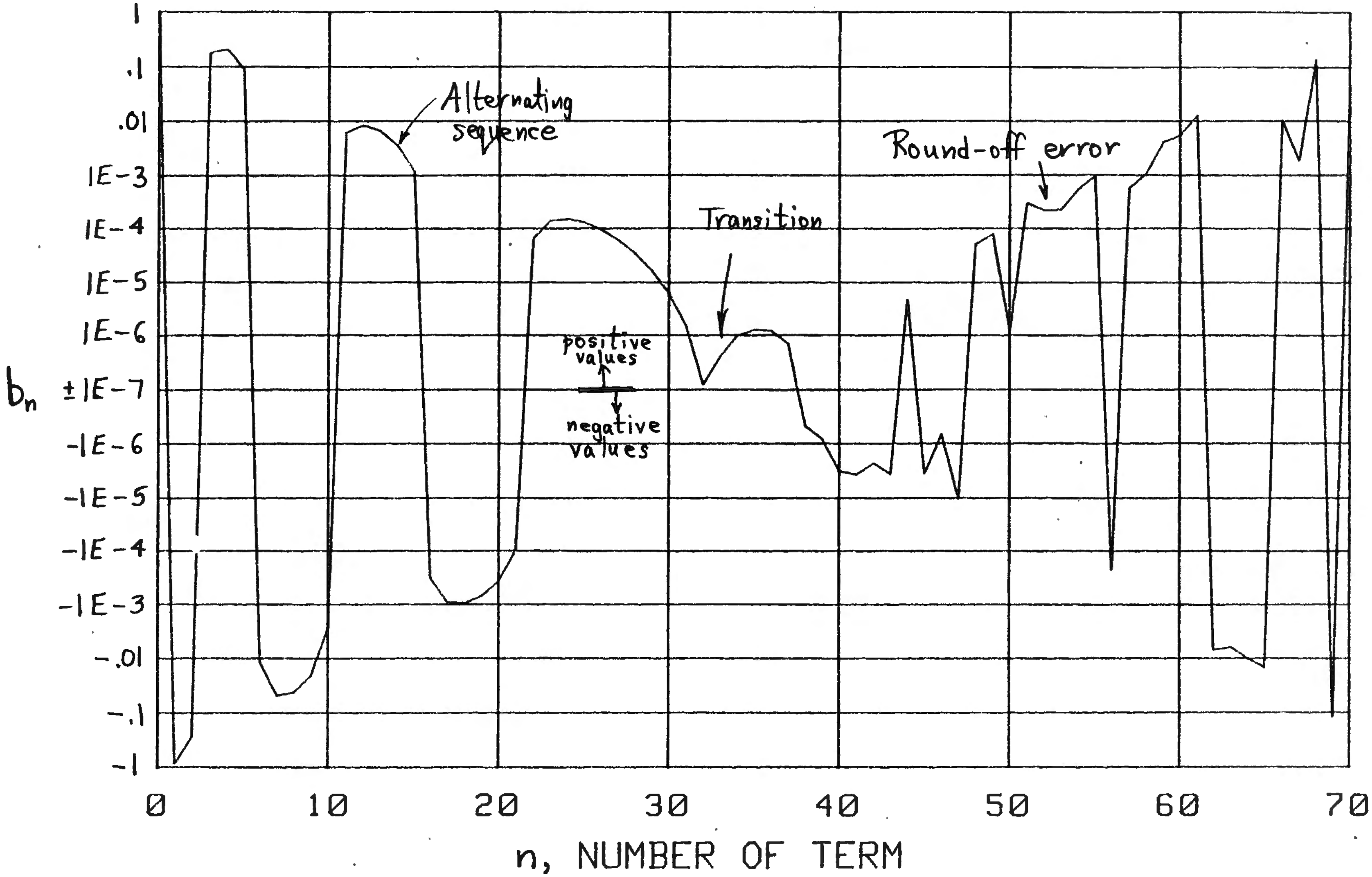

Figure D-1. Coefficient b_n in Laguerre Expansion

```
10 !   STEP PLUS CONTINUOUS PART OF SHOT NOISE CDF, Pc(u),
20 !   VIA GENERALIZED LAGUERRE EXPANSION AND MOMENTS
30     M=70   !  MAXIMUM ORDER OF APPROXIMATION; NUMBER OF MOMENTS REQUIRED
40     DOUBLE M,I,N,K                    !  INTEGERS < 2^31 = 2,147,483,648
50     REDIM Mom(0:M),A(0:M),L(0:M)
60     REAL Mom(0:100),A(0:100),L(0:100),Y(1:21)
70     CALL Moments(M,P0,Mom(*))         !  P0 IS STEP AT ORIGIN
80     Center=Mom(1)/Mom(0)              !  CENTER OF pc(u)
90     R2=Mom(2)/Mom(0)-Center*Center    !  MEAN SQUARE SPREAD OF pc(u)
100    Rms=SQR(R2)                       !  RMS SPREAD OF pc(u)
110    Alpha0=Center*Center/R2-1.        !  THE CHOICES   Alpha=Alpha0    AND
120    Beta0=R2/Center                   !  Beta=Beta0   WOULD MAKE A(1)=A(2)=0
130      Alpha=.74
140      Beta=2.1
150    CALL Coeffld_via_mom(M,Alpha,Beta,Mom(*),A(*))    !   DIRECT    MOMENTS
160  ! CALL Coefflr_via_mom(M,Alpha,Beta,Mom(*),A(*))    !   RECURSIVE MOMENTS
170    PRINT "Center = ";Center
180    PRINT "Rms =";Rms
190    A1=Alpha+1.
200    O1=1./A1
210    F1=1./FNGamma(A1)
220    DATA .001,.002,.005,.01,.02,.05,.1,.2,.3,.4,.5
230    DATA .6,.7,.8,.9,.95,.98,.99,.995,.998,.999
240    READ Y(*)
250    FOR I=1 TO 21
260    Y(I)=FNInvphi(Y(I))
270    NEXT I
280    Y1=Y(1)
290    Y2=Y(21)
300      INPUT "ORDER AND LIMITS:",N,U1,U2
310    PRINT "ORDER AND LIMITS:",N;U1;U2
320    Du=(U2-U1)/100.
330    PLOTTER IS "GRAPHICS"
340    GRAPHICS ON
350    WINDOW U1,U2,Y1,Y2
360    FOR U=U1 TO U2 STEP (U2-U1)*.1
370    MOVE U,Y1
380    DRAW U,Y2
390    NEXT U
400    FOR I=1 TO 21
410    MOVE U1,Y(I)
420    DRAW U2,Y(I)
430    NEXT I
440    PENUP
450    FOR I=1 TO 100
460    U=U1+Du*I
470    T=U/Beta
480    CALL Laguerre(N-1,A1,T,L(*))
490    Sum=A(0)*FNF11(A1,T)*O1
500    FOR K=1 TO N
510    Sum=Sum+A(K)*L(K-1)/K
520    NEXT K
530    P=P0+F1*EXP(-T+A1*LOG(T))*Sum     !  PROBABILITY THAT RV < U
540    IF P>0. AND P<1. THEN 570
550    PENUP
560    GOTO 580
570    PLOT U,FNInvphi(P)
580    NEXT I
590    PENUP
600    GOTO 300
610    END
620    !
```

```
 630    DEF FNInvphi(X)  !  INVPHI(X) via 26.2.23 with modification
 640    D=X-.5
 650    IF ABS(D)>.01 THEN 680
 660    P=2.50662827463*D*(1.+D*D*1.04719755120)
 670    RETURN P
 680    P=X
 690    IF X>.5 THEN P=1.-X
 700    P=SQR(-2.*LOG(P))
 710    T=1.+P*(1.432788+P*(.189269+P*.001308))
 720    P=P-(2.515517+P*(.802853+P*.010328))/T
 730    IF X<.5 THEN P=-P
 740    RETURN P
 750    FNEND
 760    !
 770    DEF FNGamma(X)  !  Gamma(X) via HART, page 282, #5243
 780    DOUBLE N,K
 790    N=INT(X)
 800    R=X-N
 810    IF N>0 OR R<>0. THEN 840
 820    PRINT "FNGamma(X) IS NOT DEFINED FOR X = ";X
 830    STOP
 840    IF R>0. THEN 870
 850    Gamma2=1.
 860    GOTO 940
 870    P=439.33044060025676+R*(50.1086937529709530+R*6.74495072459252899)
 880    P=8762.71029785214896+R*(2008.52740130727912+R*P)
 890    P=42353.6895097440896+R*(20886.8617892698874+R*P)
 900    Q=499.028526621439048-R*(189.498234157028016-R*(23.081551524580125-R))
 910    Q=9940.30741508277090-R*(1528.60727377952202+R*Q)
 920    Q=42353.6895097440900+R*(2980.38533092566499-R*Q)
 930    Gamma2=P/Q                       !  Gamma(2+R) for 0 < R < 1
 940    IF N>2 THEN 980
 950    IF N<2 THEN 1030
 960    Gamma=Gamma2
 970    RETURN Gamma
 980    Gamma=Gamma2
 990    FOR K=1 TO N-2
1000    Gamma=Gamma*(X-K)
1010    NEXT K
1020    RETURN Gamma
1030    R=1.
1040    FOR K=0 TO 1-N
1050    R=R*(X+K)
1060    NEXT K
1070    Gamma=Gamma2/R
1080    RETURN Gamma
1090    FNEND
1100    !
```

```
1110    DEF FNF11(A1,X)                     !  1F1(1;A1+1;X)
1120    DOUBLE K
1130    T=S=1.
1140    FOR K=1 TO 200
1150    T=T*X/(A1+K)
1160    S=S+T
1170    IF T<=1.E-17*S THEN RETURN S
1180    NEXT K
1190    PRINT "200 TERMS IN FNF11 AT";A1;X
1200    RETURN S
1210    FNEND
1220    !
1230    SUB Laguerre(DOUBLE N,REAL Alpha,X,L(*))   !  Ln\alpha(X)
1240    DOUBLE K
1250    A1=Alpha-1.
1260    L(0)=1.
1270    L(1)=Alpha+1.-X
1280    FOR K=2 TO N
1290    L(K)=((K+K+A1-X)*L(K-1)-(K+A1)*L(K-2))/K
1300    NEXT K
1310    SUBEND
1320    !
1330    SUB Momnt_via_cumnt(DOUBLE M,REAL Cum(*),Mom(*))
1340    DOUBLE K,J
1350    REAL Mom0
1360    Mom(0)=Mom0=EXP(Cum(0))
1370    FOR K=1 TO M
1380    T=1.
1390    S=Cum(K)*Mom0
1400    FOR J=1 TO K-1
1410    T=T*(K-J)/J
1420    S=S+T*Cum(K-J)*Mom(J)
1430    NEXT J
1440    Mom(K)=S
1450    NEXT K
1460    SUBEND
1470    !
```

```
1480    SUB Coeffld_via_mom(DOUBLE M,REAL Alpha,Beta,Mom(*),A(*))
1490    ALLOCATE B(0:M)
1500    DOUBLE K,K1,J,Mx
1510    T=1.
1520    FOR K=1 TO M
1530    T=T*(Alpha+K)*Beta
1540    Mom(K)=Mom(K)/T    !  NORMALIZED MOMENTS, RELATIVE TO Alpha AND Beta
1550    NEXT K
1560    Q=1.
1570    A(0)=B(0)=Mom(0)
1580    FOR K=1 TO M
1590    K1=K+1
1600    T=1.
1610    S=Mom(0)
1620    FOR J=1 TO K
1630    T=T*(J-K1)/J
1640    S=S+T*Mom(J)
1650    NEXT J
1660    Q=Q*(Alpha+K)/K
1670    A(K)=S
1680    B(K)=S*SQR(Q)
1690    NEXT K
1700    Mx=Mx+10
1710    IF Mx<M THEN 1700
1720    Threshold=-7.
1730    T2=Threshold*2.
1740    V=10.^Threshold
1750    GINIT
1760    PLOTTER IS "GRAPHICS"
1770    GRAPHICS ON
1780    WINDOW 0.,FLT(Mx),T2,0.
1790    LINE TYPE 3
1800    FOR J=0 TO Mx STEP 10
1810    MOVE J,T2
1820    DRAW J,0.
1830    NEXT J
1840    FOR J=T2 TO 0
1850    MOVE 0.,J
1860    DRAW Mx,J
1870    NEXT J
1880    PENUP
1890    LINE TYPE 1
1900    IMAGE 4D,2(4X,M.17DE)
1910    PRINT "   K                B(K)                          Sum"
1920    Sum=0.
1930    FOR K=0 TO M
1940    B=B(K)
1950    Sum=Sum+B*B
1960    PRINT USING 1900;K,B,Sum
1970    IF B<V THEN 2000
1980    Y=LGT(B)
1990    GOTO 2040
2000    IF B>-V THEN 2030
2010    Y=T2-LGT(-B)
2020    GOTO 2040
2030    Y=Threshold
2040    PLOT K,Y
2050    NEXT K
2060    PENUP
2070    SUBEND
2080    !
```

```
2090    SUB Coefflr_via_mom(DOUBLE M,REAL Alpha,Beta,Mom(*),A(*))
2100    ALLOCATE B(0:M)
2110    DOUBLE K,K1,J,Mx
2120    T=1.
2130    FOR K=1 TO M
2140    T=T*(Alpha+K)*Beta
2150    Mom(K)=Mom(K)/T   !  NORMALIZED MOMENTS, RELATIVE TO Alpha AND Beta
2160    NEXT K
2170    Q=1.
2180    A0=A(0)=B(0)=Mom(0)
2190    FOR K=1 TO M
2200    K1=K+1
2210    T=1.
2220    S=Mom(K)-A0
2230    FOR J=1 TO K-1
2240    T=T*(J-K1)/J
2250    S=S-T*A(J)
2260    NEXT J
2270    IF K MOD 2=1 THEN S=-S
2280    Q=Q*(Alpha+K)/K
2290    A(K)=S
2300    B(K)=S*SQR(Q)
2310    NEXT K
2320    Mx=Mx+10
2330    IF Mx<M THEN 2320
2340    Threshold=-7.
2350    T2=Threshold*2.
2360    V=10.^Threshold
2370    GINIT
2380    PLOTTER IS "GRAPHICS"
2390    GRAPHICS ON
2400    WINDOW 0.,FLT(Mx),T2,0.
2410    LINE TYPE 3
2420    FOR J=0 TO Mx STEP 10
2430    MOVE J,T2
2440    DRAW J,0.
2450    NEXT J
2460    FOR J=T2 TO 0
2470    MOVE 0.,J
2480    DRAW Mx,J
2490    NEXT J
2500    PENUP
2510    LINE TYPE 1
2520    IMAGE 4D,2(4X,M.17DE)
2530    PRINT "    K                B(K)                              Sum"
2540    Sum=0.
2550    FOR K=0 TO M
2560    B=B(K)
2570    Sum=Sum+B*B
2580    PRINT USING 2520;K,B,Sum
2590    IF B<V THEN 2620
2600    Y=LGT(B)
2610    GOTO 2660
2620    IF B>-V THEN 2650
2630    Y=T2-LGT(-B)
2640    GOTO 2660
2650    Y=Threshold
2660    PLOT K,Y
2670    NEXT K
2680    PENUP
2690    SUBEND
2700    !
```

```
2710    SUB Moments(DOUBLE M,REAL P0,Mom(*))        !  SHOT NOISE
2720    Overlap=6.2               !  AV. NO. PULSES/SEC * AVERAGE PULSE DURATION
2730    Sigmaa=1.                 !  PARAMETER OF RAYLEIGH AMPLITUDE PDF
2740    P0=EXP(-Overlap)          !  PROBABILITY OF ZERO AMPLITUDE OF SHOT NOISE
2750    ALLOCATE Cum(0:M)         !  ARRAY FOR CUMULANTS
2760    DOUBLE K
2770    S=Sigmaa*Sigmaa
2780    Cum(0)=0.
2790    Cum(1)=Overlap*Sigmaa*.25*PI*SQR(.5*PI)
2800    Cum(2)=Overlap*S*4./3.
2810    FOR K=3 TO M
2820    Cum(K)=Cum(K-2)*S*K*K/(K+1)
2830    NEXT K
2840    CALL Momnt_via_cumnt(M,Cum(*),Mom(*))
2850    Mom(0)=Mom(0)-P0
2860    SUBEND
```

```
 10 !  CONTINUOUS PART OF SHOT NOISE PDF, pc(u), VIA
 20 !  GENERALIZED LAGUERRE EXPANSION AND MOMENTS
 30    M=90   !  MAXIMUM ORDER OF APPROXIMATION; NUMBER OF MOMENTS REQUIRED
 40    DOUBLE M,I,N,K                     !  INTEGERS < 2^31 = 2,147,483,648
 50    REDIM Mom(0:M),A(0:M),L(0:M)
 60    REAL Mom(0:100),A(0:100),L(0:100)
 70    CALL Moments(M,P0,Mom(*))          !  P0 IS STEP AT ORIGIN
 80    Center=Mom(1)/Mom(0)               !  CENTER OF pc(u)
 90    R2=Mom(2)/Mom(0)-Center*Center     !  MEAN SQUARE SPREAD OF pc(u)
100    Rms=SQR(R2)                        !  RMS SPREAD OF pc(u)
110    Alpha0=Center*Center/R2-1.         !  THE CHOICES   Alpha=Alpha0    AND
120    Beta0=R2/Center                    !  Beta=Beta0   WOULD MAKE A(1)=A(2)=0
130      Alpha=.74
140      Beta=2.1
150    CALL Coeffld_via_mom(M,Alpha,Beta,Mom(*),A(*))    !   DIRECT    MOMENTS
160  ! CALL Coefflr_via_mom(M,Alpha,Beta,Mom(*),A(*))    !   RECURSIVE MOMENTS
170    PRINT "Center = ";Center
180    PRINT "Rms =";Rms
190    F1=1./(Beta*FNGamma(Alpha+1.))
200      INPUT "ORDER AND LIMITS:",N,U1,U2
210    PRINT "ORDER AND LIMITS:",N;U1;U2
220    Du=(U2-U1)/100.
230    H=4./(U2-U1)
240    PLOTTER IS "GRAPHICS"
250    GRAPHICS ON
260    WINDOW U1,U2,-H*.1,H
270    GRID (U2-U1)*.1,H*.1
280    PLOT 0.,0.
290    FOR I=1 TO 100
300    U=U1+Du*I
310    T=U/Beta
320    CALL Laguerre(N,Alpha,T,L(*))
330    Sum=A(0)
340    FOR K=1 TO N
350    Sum=Sum+A(K)*L(K)
360    NEXT K
370    P=F1*EXP(-T+Alpha*LOG(T))*Sum   !   PDF OF RV AT U
380    PLOT U,P
390    NEXT I
400    PENUP
410    GOTO 200
420    END
430    !
```

REFERENCES

1. S. O. Rice, "Mathematical Analysis of Random Noise," Bell System Technical Journal, vols. 23 and 24, 1945. Also in Noise and Stochastic Processes, edited by N. Wax, Dover Publications, N.Y., 1954.

2. Handbook of Mathematical Functions, National Bureau of Standards, Applied Math Series, No. 55, U.S. Dept. of Comm., U.S. Govt. Printing Office, Wash. D.C., June 1964.

3. H. Cramér, Mathematical Methods of Statistics, Princeton University Press, 1961.

4. A. H. Nuttall, "Determination of Densities and Distributions via Hermite and Generalized Laguerre Expansions, Employing High-Order Recursive Cumulants or Moments," NUSC Technical Report, to be published.

5. I. S. Gradshteyn and I. M. Ryzhik, Table of Integrals, Series, and Products, Academic Press Inc., N.Y., 1980.

6. A. H. Nuttall, "Recursive Inter-Relationships Between Moments, Central Moments, and Cumulants," NUSC Technical Memorandum TC-201-71, 12 October 1971.

7. A. H. Nuttall and B. Dedreux, "Exact Operating Characteristics for Linear Sum of Envelopes of Narrowband Gaussian Process and Sinewave," NUSC Technical Report 7117, 11 January 1984.